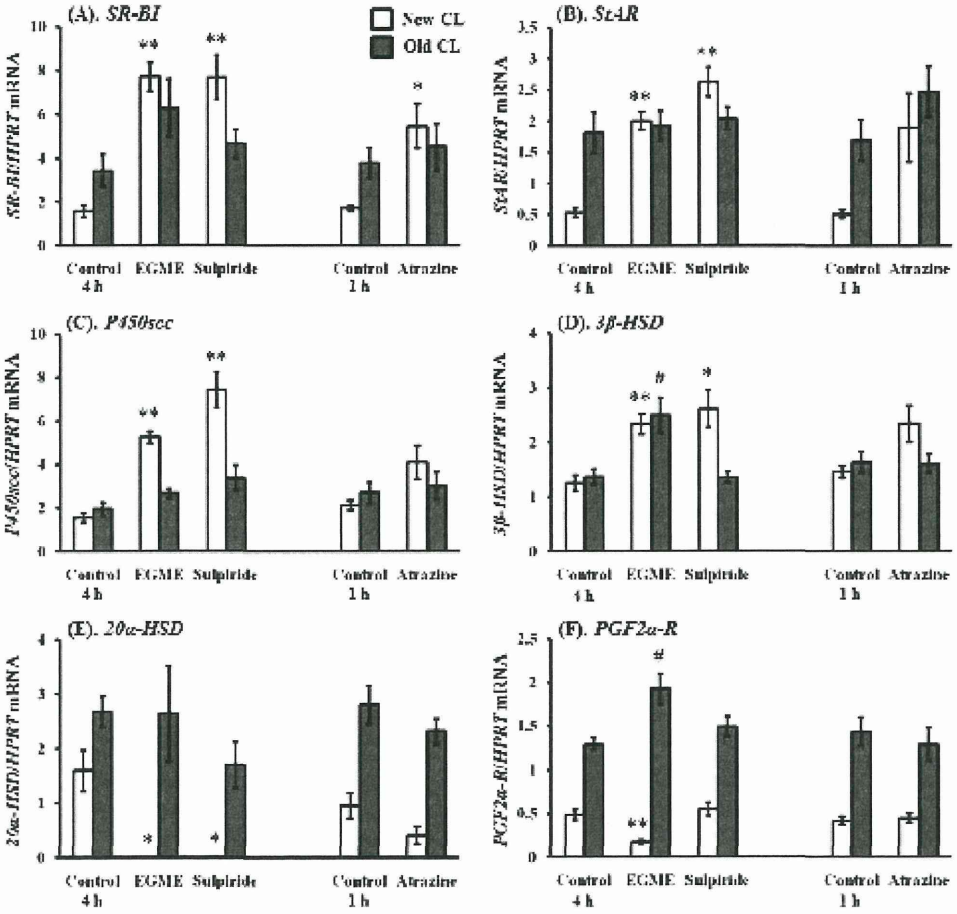

FIG. 3. Effects of EGME, sulpiride, or atrazine on gene expression levels of steroidogenic and luteolytic factors in new and old CL. Relative mRNA levels of *SR-BI* (A), *StAR* (B), *P450scc* (C), *3β-HSD* (D), *20α-HSD* (E), and *PGF2α-R* (F) are presented. Animals were euthanized at 4 h (EGME and sulpiride) or 1 h (atrazine) after the last dose ($n = 4$–5). Data are normalized for *HPRT* mRNA levels in each sample and presented as the mean ± SEM, with asterisks and hashes indicating significant differences as compared with the controls (**$p < 0.01$, *$p < 0.05$, #$p < 0.05$).

Of the other genes related to steroidogenesis, both types of *PRL-R* (*Long* and *Short forms*) genes were significantly increased in new and old CL of the EGME group and new CL of the sulpiride group (Figs. 4A and 4B). The most drastic change was an increased *NR5A2* mRNA level in new CL of the EGME (8.7-fold) and sulpiride (13.4-fold) groups (Fig. 4D). The *ACAT-1* mRNA levels in new CL of the EGME and sulpiride groups were significantly higher than those of the control group (Fig. 4E). In the atrazine-treated CL, there was a trend to higher mRNA levels of *SF-1* and *ACAT-1* mRNA in the new CL; however, this was not significant (Figs. 4C and 4E).

Morphometric analysis of the immunohistochemical staining of steroidogenic factors in new and old CL. There were no histopathological changes in the HE-stained specimens in any of the treatment groups compared with the controls following daily four times of treatment (data not shown). In the analysis of the SR-BI-, StAR-, P450scc-, and 3β-HSD-positive luteal cells in new and old CL (Fig. 5 and Supplementary figs. 2 and 3), the

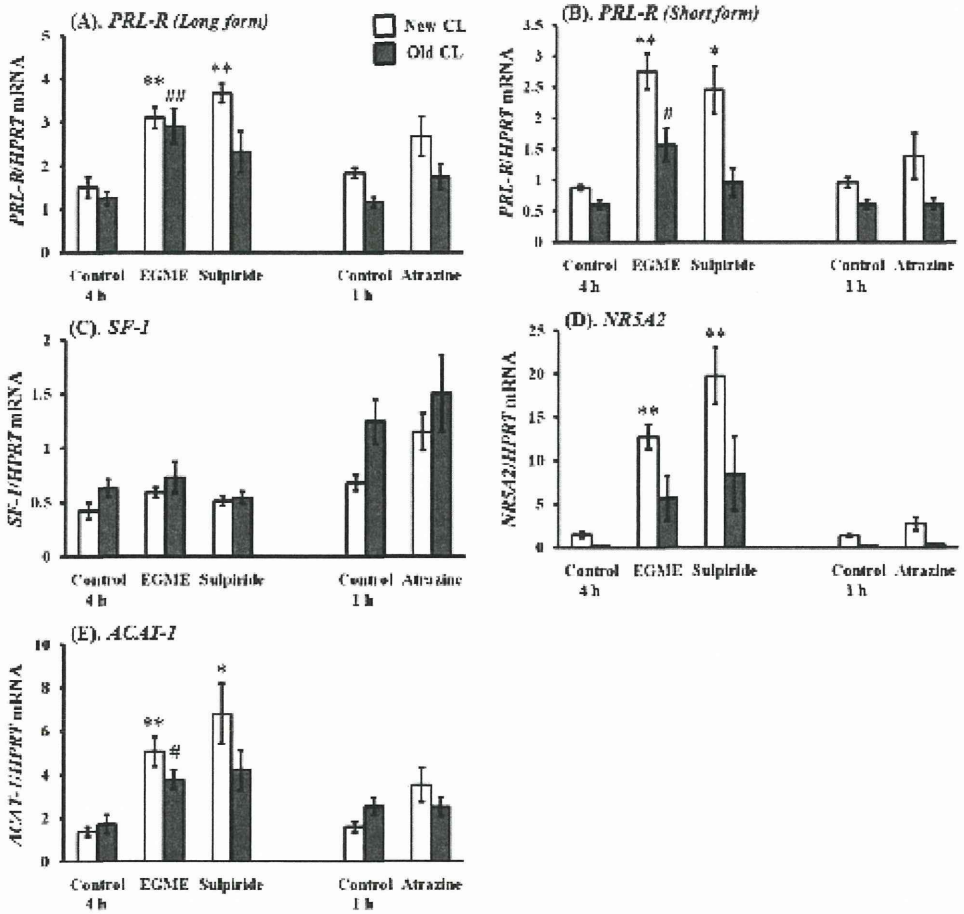

FIG. 4. Effects of EGME, sulpiride, or atrazine on gene expression levels of *PRL-R (Long form)* (A), *PRL-R (Short form)* (B), *SF-1* (C), *NR5A2* (D), and *ACAT-1* (E) in new and old CL. Animals were euthanized at 4 h (EGME and sulpiride) or 1 h (atrazine) after the last dose ($n = 4$–5). Data were normalized for *HPRT* mRNA levels in each sample and presented as the mean ± SEM, with asterisks and hashes indicating significant differences as compared with the controls (**$p < 0.01$, *$p < 0.05$, ##$p < 0.01$, #$p < 0.05$).

integrated density was mostly higher in new CL than in old CL. New CL in all treatment groups showed significantly higher intensities of these four steroidogenic factors. In comparison to the respective controls, SR-BI and StAR were significantly higher in all treatment groups (up to 2.0- and 6.1-fold in SR-BI and StAR, respectively), P450scc in the EGME and sulpiride groups (up to 1.9-fold), and 3β-HSD in the EGME and atrazine groups (up to 1.6-fold) (Figs. 5A–D). Intensities of the four steroidogenic factors in old CL also showed a higher tendency in all treatment groups and were significantly higher for SR-BI in the atrazine group (1.5-fold), P450scc in the EGME and sulpiride groups (1.9-fold), and 3β-HSD in the EGME group (1.8-fold) in comparison to the controls (Figs. 5A, 5C, and 5D).

Experiment 3

Alterations of serum hormone concentrations. Serum P4 levels were significantly higher in the EGME (2.7-fold) and EGME + BRC (2.0-fold) groups compared with those in the control groups (Fig. 6A). The PRL level was significantly higher in the EGME group (2.7-fold) and tended to be lower

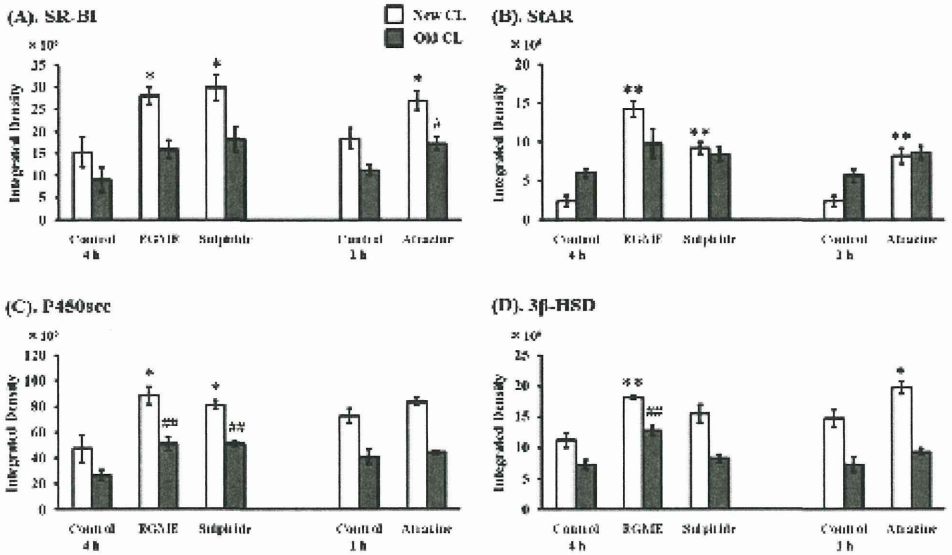

FIG. 5. Effects of EGME, sulpiride, or atrazine on immunoreactivities of steroidogenic factors in new and old CL. Integrated densities of SR-BI (A), StAR (B), P450scc (C), and 3β-HSD (D) are presented. Animals were euthanized at 4 h (EGME and sulpiride) or 1 h (atrazine) after the last dose ($n = 4$–5). Data were presented as the mean ± SEM, with asterisks and hashes indicating significant differences as compared with the controls (**$p < 0.01$, *$p < 0.05$, ##$p < 0.01$, #$p < 0.05$).

in the BRC (0.1-fold) and EGME + BRC (0.05-fold) groups in comparison to the controls (Fig. 6B). No significant difference was observed in E_2, LH, and FSH levels (data not shown).

Changes of steroidogenic and luteolytic gene expressions in new and old CL. In new CL of the EGME and EGME + BRC groups, mRNA expression levels of steroidogenic factors were significantly higher ($p < 0.01$ or 0.05) and those of luteolytic factors were significantly lower ($p < 0.01$) than in the control group, though the effect was less pronounced with combined BRC treatment (Figs. 7A–F). In contrast, BRC treatment alone significantly increased the *20α-HSD* mRNA level in new CL ($p < 0.01$) (Fig. 7E). In old CL, mRNA levels of *SR-BI* in the EGME and EGME + BRC groups, *P450scc* and *PGF2α-R* in the EGME group, and *3β-HSD* in the EGME + BRC group were significantly increased ($p < 0.01$ or 0.05) (Figs. 7A, 7C, 7D, and 7F).

For the other steroidogenesis-related genes, both forms of *PRL-R*, *NR5A2*, and *ACAT-1* mRNA levels were significantly increased in new and old CL in the EGME group and in new CL of the EGME + BRC group ($p < 0.01$ or 0.05) (Figs. 8A–D). Cotreatment of EGME and BRC also increased *PRL-R* (*Long form*) mRNA in old CL (Fig. 8A). No significant changes in these genes were observed in the BRC group.

Morphometric analysis of the immunohistochemical staining of steroidogenic factors in new and old CL. There were no

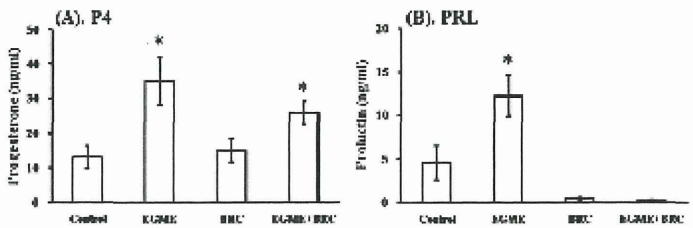

FIG. 6. Serum hormone levels after four daily treatments of EGME, BRC, or EGME and BRC. Data represent serum P4 (A) and PRL (B) levels (mean ± SEM). Animals were euthanized 4 h after the last dose ($n = 4$–5). Asterisk ($p < 0.05$) indicates significant differences as compared with the controls.

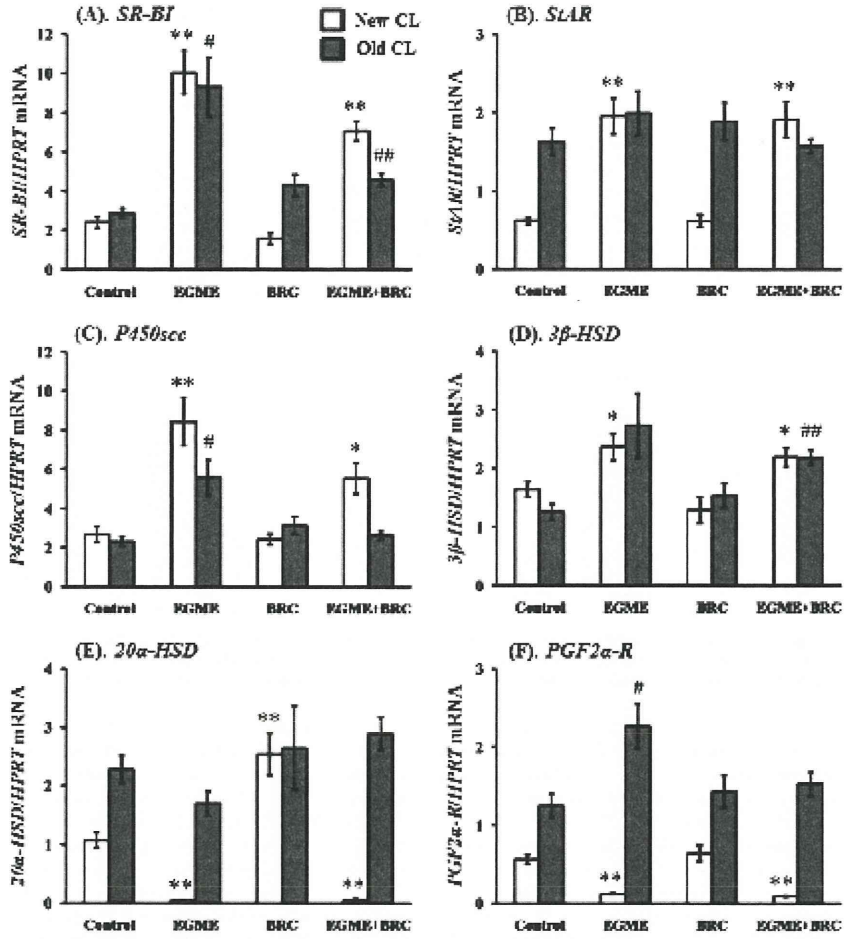

FIG. 7. Effects of EGME, BRC, or EGME and BRC on gene expression levels of steroidogenic and luteolytic factors in new and old CL. Relative mRNA levels of *SR-BI* (A), *StAR* (B), *P450scc* (C), *3β-HSD* (D), *20α-HSD* (E), and *PGF2α-R* (F) are presented. Animals were euthanized 4 h after the last dose ($n = 4$–5). Data are normalized for *HPRT* mRNA levels in each sample and presented as the mean ± SEM, with asterisks and hashes indicating significant differences as compared with the controls (**$p < 0.01$, *$p < 0.05$, ##$p < 0.01$, #$p < 0.05$).

histopathological changes in the HE-stained specimens following any of the treatments in comparison to the control (data not shown). New CL in the EGME and EGME + BRC groups showed higher intensities of SR-BI, StAR, and P450scc; intensities were significantly higher for StAR in both groups (up to 5.1-fold), SR-BI in the EGME group (1.3-fold), and P450scc in the EGME + BRC group (1.4-fold) in comparison to the controls (Figs. 9A–C). SR-BI was significantly higher in old CL of the EGME + BRC group (1.4-fold) (Fig. 9A). In the BRC group, significantly lower staining intensities were observed in new CL for StAR and 3β-HSD and old CL for 3β-HSD (Figs. 9B and 9D).

DISCUSSION

The focus of this study was to clarify the toxicological pathways by which three ovarian toxicants, EGME, sulpiride,

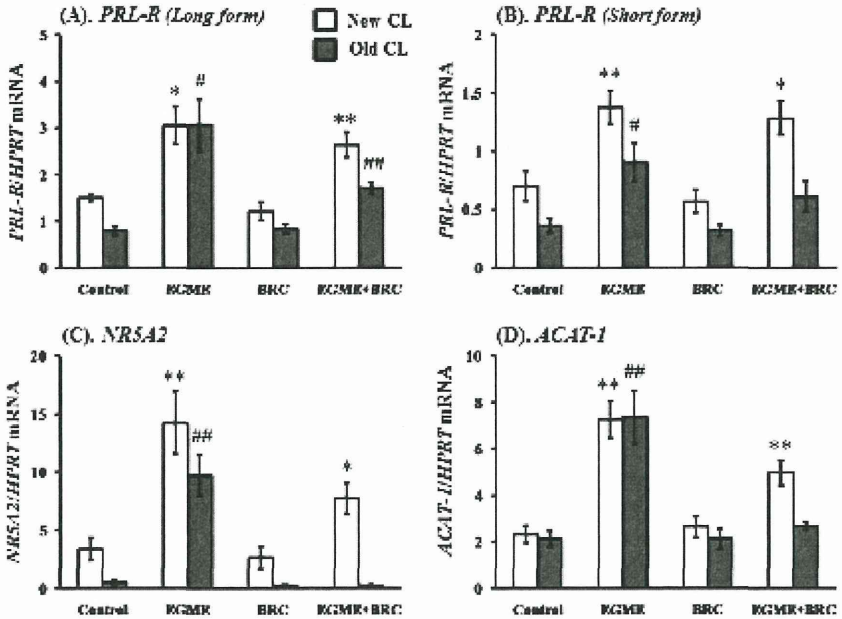

FIG. 8. Effects of EGME, BRC, or EGME and BRC on gene expression levels of *PRL-R (Long form)* (A), *PRL-R (Short form)* (B), *NR5A2* (C), and *ACAT-1* (D) in new and old CL. Animals were euthanized 4 h after the last dose ($n = 4$–5). Data were normalized for *HPRT* mRNA levels in each sample and presented as the mean ± SEM, with asterisks and hashes indicating significant differences as compared with the controls (**$p < 0.01$, *$p < 0.05$, ##$p < 0.01$, #$p < 0.05$).

and atrazine, affected luteal steroidogenesis in new and old CL *in vivo*. In the present study, all compounds significantly increased the serum P4 level secondary to upregulated expression levels of all steroidogenic factors and downregulation of the *20α-HSD* gene in new CL. The serum E_2, LH, and FSH levels were not altered. Two weeks of treatment with EGME, sulpiride, or atrazine induced similar histopathological changes in luteal cells to what has been previously reported (Davis *et al.*, 1997; Dodo *et al.*, 2009; Shibayama *et al.*, 2009; Yuan and Foley, 2002). These histopathological changes reflect the activation of luteal cells and are associated with increased P4 production activity (Davis *et al.*, 1997; Fraites *et al.*, 2009; Ishii *et al.*, 2009). The present short-term study provides new evidence that new CL are the main targets of these compounds.

EGME as well as sulpiride, a compound which stimulates PRL secretion, increased the serum PRL level in the present study. This is in contrast to a previous study showing suppression of PRL secretion following EGME treatment of female rats (Davis *et al.*, 1997). Although the reason of this discrepancy is unclear, our results represent new evidence that EGME, via the HPG axis, indirectly stimulates luteal pathways in the ovary. This conclusion is further strengthened by the results following coadministration of BRC with EGME, which will be discussed subsequently.

The results of experiment 2 indicate that the gene expression changes of steroidogenic factors correspond to the changes in the immunohistochemical intensities of the factors in new and old CL. The increases in *SR-BI*, *StAR*, *P450scc*, and *3β-HSD* mRNA levels and immunohistochemical intensity levels in new CL following four daily treatments with any of the three compounds represent stimulation of steroidogenesis with resulting P4 production in new CL. Additionally, the increase in *3β-HSD* expression both at the gene transcription and protein expression levels in old CL following treatment with EGME indicates that EGME stimulates steroidogenesis in old CL. Although increases in steroidogenic gene expression were not produced by treatment with the other compounds, a trend to increased immunoreactivity was seen, suggesting that sulpiride and atrazine may also stimulate steroidogenesis in old CL.

The decreases of the luteolytic factor *20α-HSD* mRNA in the new CL from all treatment groups and *PGF2α-R* mRNA in the new CL from the EGME group clearly demonstrate the inhibition of catabolism of P4 into 20α-DHP, indicating a higher P4 production ability in new CL. These results demonstrate that not only promotion of steroidogenesis but also suppression of P4 catabolism in new CL is directly or indirectly induced by EGME, sulpiride, or atrazine treatment.

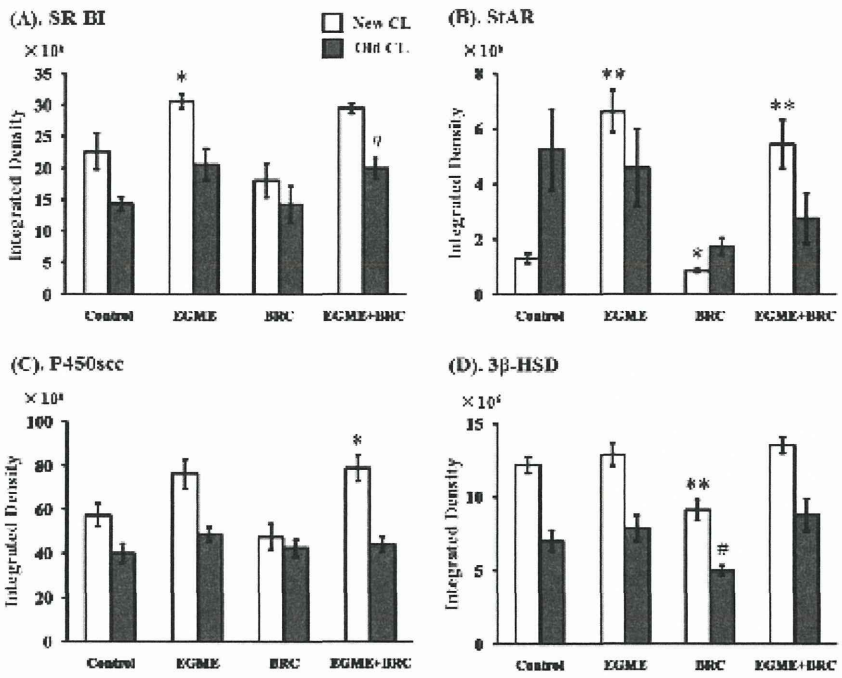

FIG. 9. Effects of EGME, BRC, or EGME and BRC on the immunoreactivities of steroidogenic factors in new and old CL. Integrated densities of SR-BI (A), StAR (B), P450scc (C), and 3β-HSD (D) are presented. Animals were euthanized 4 h after the last dose ($n = 4$–5). Data are presented as the mean ± SEM, with asterisks and hashes indicating significant differences as compared with the controls (**$p < 0.01$, *$p < 0.05$, #$p < 0.05$).

Consistent with the role of PRL as an upregulator of steroidogenic factors and a downregulator of 20α-HSD in the rat ovary (Stocco *et al.*, 2007), the present study clearly showed that the stimulation of P4 secretion by sulpiride was caused by increased PRL secretion. The concurrent administration of EGME with BRC, a D2 agonist, in experiment 3 demonstrated that EGME stimulated P4 secretion, upregulated steroidogenic factor expression levels, and downregulated luteolytic factor expression levels in new CL without PRL hypersecretion. These findings taken in the context of consistent observations *in vitro* (Almekinder *et al.*, 1997; Davis *et al.*, 1997) suggest that EGME has a direct luteal stimulatory effect *in vivo*. Although the immunohistochemical intensities of P450scc and 3β-HSD in new and old CL of EGME group were significantly higher than controls in experiment 2, there was no significant change between them in experiment 3. These inconsistencies were attributed to differences in the conditions for tissue fixation; ovaries were fixed in 4% paraformaldehyde and 10% vol neutral-buffered formalin in experiments 2 and 3, respectively.

In other steroidogenesis-related genes, increases in both forms of *PRL-R* in new CL following EGME or sulpiride treatment may reflect increased PRL secretion because they have been upregulated in pregnant female rats (Dunaif *et al.*, 1982; Telleria *et al.*, 1997). Additionally, EGME and sulpiride remarkably increased *NR5A2* mRNA level in new CL. *NR5A2* is a crucial factor in PRL-regulated P4 secretion (Falender *et al.*, 2003; Labelle-Dumais *et al.*, 2007; Liu *et al.*, 2003; Saxena *et al.*, 2007). Therefore, the increased expression of the *NR5A2* gene might be related to the PRL-stimulating effect of EGME and sulpiride. Because the *SF-1* gene, which belongs to the same nuclear receptor family as *NR5A2*, regulates the E_2 and P4 synthesis in granulosa cells (Falender *et al.*, 2003; Saxena *et al.*, 2007), its expression in CL did not change in any treatment groups. Upregulation of the *ACAT-1* gene, which contributes to the storage of free cholesterol in lipid droplets in luteal cells (Stouffer, 2006), was also observed in new and old CL following the EGME or sulpiride treatment. This change seems to contribute the histopathological luteal hypertrophy by repeated administration of these compounds. Intriguingly, coadministration of EGME and BRC produced similar changes in gene expression levels of *PRL-R*, *NR5A2*, and *ACAT-1* in new CL. These observations allude to the possibility that the direct luteal stimulation mechanism of EGME is similar to PRL

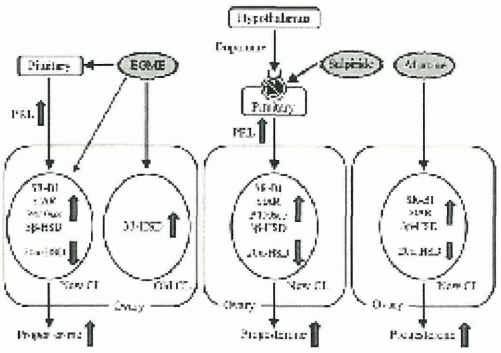

FIG. 10. Overview of the luteal effects of EGME, sulpiride, and atrazine. EGME upregulates steroidogenic factor expressions and downregulates luteolytic factor expression. This results in an increase in P4 secretion from new CL by both direct and indirect (PRL dependent) pathways. EGME also directly stimulates the expression of 3β-HSD in old CL. Sulpiride stimulates PRL secretion sustainably by suppressing the dopaminergic activity in the anterior pituitary. This results in the activation of new CL and increased P4 secretion. Atrazine also stimulates P4 secretion in new CL by upregulating SR-BI, StAR, and 3β-HSD expression levels and downregulating 20α-HSD expression level. Gray arrows represent the increases or decreases of the luteal gene/protein expression levels or hormone secretion.

dependent stimulation pattern. Thus, two pathways likely mediate the luteal stimulatory effect of EGME on the ovary and consist of a direct pathway and an indirect pathway, which depends on PRL hypersecretion.

Previous reports have described a neuroendocrine effect of atrazine in rats. Atrazine inhibits the preovulatory surge of LH and PRL by disrupting the hypothalamic control (Cooper *et al.*, 2000; Foradori *et al.*, 2009). Although these reports explain the disruption of estrous cyclicity by atrazine treatment, the cause of the increased P4 level cannot be explained by these observations. Fraites *et al.* (2009) and Laws *et al.* (2009), however, recently reported that atrazine or its chlorinated metabolite, desisopropylatrazine, increased circulating P4 levels by activating the hypothalamic-pituitary-adrenal axis in male and female rats. The present results demonstrated no increase in serum PRL level following atrazine treatment. In addition, no morphological change was observed in the adrenals in the present study, suggesting a possibility of a direct stimulatory effect of atrazine on CL. Because the ovary is the main site of P4 secretion in female rats, P4 production from the adrenal likely does not represent a significant target of atrazine treatment in female.

With regard to the other steroidogenesis-related genes (*PRLR*, *NR5A2*, and *ACAT-1*), the lack of change in expression levels following atrazine treatment suggests that its mechanism differs from that of EGME or sulpiride. Atrazine has been shown to increase the concentration of cyclic adenosine monophosphate (cAMP) (Sanderson *et al.*, 2002), inhibit phosphodiesterase (Roberge *et al.*, 2006), induce *P450scc* gene expression, and activate phosphatidylinositol 3-kinase (PI3K) signaling cascades (Suzawa and Ingraham, 2008) *in vitro*. The present study did not confirm any of these findings and suggests that further experiments are needed to clarify the mechanism of atrazine.

An overview of the possible pathways mediating the effects of EGME, sulpiride, or atrazine on luteal cells is summarized in Figure 10. We propose that EGME stimulates PRL secretion from the pituitary with resulting upregulation of steroidogenic factors and downregulation of luteolytic factor expression levels. This results in increased P4 secretion in new CL. In addition, EGME directly stimulates new CL in a manner similar to PRL and also directly stimulates steroidogenesis in old CL. The luteal stimulation effect of sulpiride is solely the result of disruption of the HPG axis producing hypersecretion of PRL from pituitary (indirect effect). Our results indicate that atrazine directly stimulates P4 secretion in new CL in a PRL independent manner. In conclusion, the present study provides new insights regarding the differential pathways mediating the stimulation of P4 secretion by the ovarian toxicants EGME, sulpiride, and atrazine in female rats *in vivo*. Additional studies are needed to confirm the direct effect of EGME and atrazine on luteal cells and to elucidate its mechanism.

SUPPLEMENTARY DATA

Supplementary data are available online at http://toxsci.oxfordjournals.org/.

FUNDING

Health and Labor Sciences Research Grants for Risk of Chemical Substances (No. 10103199) from the Ministry of Health, Labor, and Welfare, Japan.

ACKNOWLEDGMENTS

We thank Ms. Tomomi Morikawa, Ms. Ayako Kaneko, and Ms. Yoshimi Komatsu for their excellent technical assistance. We also appreciate Dr Satoru Hosokawa and Dr Akira Inomata (Drug Safety Japan, Global Drug Safety, Biopharmaceutical Assessments Core Function Unit, Eisai Product Creation Systems, Eisai Co., Ltd) for their helpful suggestions.

REFERENCES

Almekinder, J. L., Lennard, D. E., Walmer, D. K., and Davis, B. J. (1997). Toxicity of methoxyacetic acid in cultured human luteal cells. *Fundam. Appl. Toxicol.* **38**, 191–194.

Bowen, J. M., and Keyes, P. L. (2000). Repeated exposure to prolactin is required to induce luteal regression in the hypophysectomized rat. *Biol. Reprod.* **63**, 1179–1184.

Bridges, R. S., and Ronsheim, P. M. (1990). Prolactin (PRL) regulation of maternal behavior in rats: bromocriptine treatment delays and PRL promotes the rapid onset of behavior. *Endocrinology* **126**, 837–848.

Cooper, R. L., Laws, S. C., Das, P. C., Narotsky, M. G., Goldman, J. M., Tyrey, L., and Stoker, T. E. (2007). Atrazine and reproductive function: mode and mechanism of action studies. *Birth Defects. Res. B Dev. Reprod. Toxicol.* **80,** 98–112.

Cooper, R. L., Stoker, T. E., Tyrey, L., Goldman, J. M., and McElroy, W. K. (2000). Atrazine disrupts the hypothalamic control of pituitary-ovarian function. *Toxicol. Sci.* **53,** 297–307.

Davis, B. J., Almekinder, J. L., Flagler, N., Travlos, G., Wilson, R., and Marompot, R. R. (1997). Ovarian luteal cell toxicity of ethylene glycol monomethyl ether and methoxy acetic acid in vivo and in vitro. *Toxicol. Appl. Pharmacol.* **142,** 328–337.

Dodo, T., Taketa, Y., Sugiyama, M., Inomata, A., Sonoda, J., Okuda, Y., Mineshima, H., Hosokawa, S., and Aoki, T. (2009). Collaborative work on evaluation of ovarian toxicity. 11) Two- or four-week repeated-dose studies and fertility study of ethylene glycol monomethyl ether in female rats. *J. Toxicol. Sci.* **34,** SP121–SP128.

Dunaif, A. E., Zimmerman, E. A., Friesen, H. G., and Frantz, A. G. (1982). Intracellular localization of prolactin receptor and prolactin in the rat ovary by immunocytochemistry. *Endocrinology* **110,** 1465–1471.

Eldridge, J. C., Tennant, M. K., Wetzel, L. T., Breckenridge, C. B., and Stevens, J. T. (1994). Factors affecting mammary tumor incidence in chlortriazine-treated female rats: hormonal properties, dosage, and animal strain. *Environ. Health Perspect.* **102,** 29–36.

Eldridge, J. C., Wetzel, L. T., and Tyrey, L. (1999). Estrous cycle patterns of Sprague-Dawley rats during acute and chronic atrazine administration. *Reprod. Toxicol.* **12,** 491–499.

Falender, A. E., Lanz, R., Malenfant, D., Belanger, L., and Richards, J. S. (2003). Differential expression of steroidogenic factor-1 and FTF/LRH-1 in the rodent ovary. *Endocrinology* **144,** 3598–3610.

Foradori, C. D., Hinds, L. R., Hanneman, W. H., Legare, M. E., Clay, C. M., and Handa, R. J. (2009). Atrazine inhibits pulsatile luteinizing hormone release without altering pituitary sensitivity to a gonadotropin-releasing hormone receptor agonist in female Wistar rats. *Biol. Reprod.* **81,** 40–45.

Fraites, M. J., Cooper, R. L., Buckalew, A., Jayaraman, S., Mills, L., and Laws, S.C. (2009). Characterization of the hypothalamic-pituitary-adrenal axis response to atrazine and metabolites in the female rat. *Toxicol. Sci.* **112,** 88–99.

Hays, S. M., Elswick, B. A., Blumenthal, G. M., Welsch, F., Conolly, R. B., and Gargas, M. L. (2000). Development of a physiologically based pharmacokinetic model of 2-methoxyethanol and 2-methoxyacetic acid disposition in pregnant rats. *Toxicol. Appl. Pharmacol.* **163,** 67–74.

Ishii, S., Ube, M., Okada, M., Adachi, T., Sugimoto, J., Inoue, Y., Uno, Y., and Mutai, M. (2009). Collaborative work on evaluation of ovarian toxicity. 17) Two- or four-week repeated-dose studies and fertility study of sulpiride in female rats. *J. Toxicol. Sci.* **34,** SP175–S188.

Johanson, G. (2000). Toxicity review of ethylene glycol monomethyl ether and its acetate ester. *Crit. Rev. Toxicol.* **30,** 307–345.

Labelle-Dumais, C., Paré, J. F., Bélanger, L., Farookhi, R., and Dufort, D. (2007). Impaired progesterone production in Nr5a2+/- mice leads to a reduction in female reproductive function. *Biol. Reprod.* **77,** 217–225.

Lacruz, A., Baptista, T., de Mendoza, S., Mendoza-Guillén, J. M., and Hernández, L. (2000). Antipsychotic drug-induced obesity in rats: correlation between leptin, insulin and body weight during sulpiride treatment. *Mol. Psychiatry* **5,** 70–76.

Laws, S. C., Hotchkiss, M., Ferrell, J., Jayaraman, S., Mills, L., Modic, W., Tinfo, N., Fraites, M., Stoker, T., and Cooper, R. (2009). Chlorotriazine herbicides and metabolites activate an ACTH-dependent release of corticosterone in male Wistar rats. *Toxicol. Sci.* **112,** 78–87.

Liu, D. L., Liu, W. Z., Li, Q. L., Wang, H. M., Qian, D., Treuter, E., and Zhu, C. (2003). Expression and functional analysis of liver receptor homologue 1 as a potential steroidogenic factor in rat ovary. *Biol. Reprod.* **69,** 508–517.

McMullin, T. S., Hanneman, W. H., Cranmer, B. K., Tessari, J. D., and Andersen, M. E. (2007). Oral absorption and oxidative metabolism of atrazine in rats evaluated by physiological modeling approaches. *Toxicology* **240,** 1–14.

Rehm, S., Stanislaus, D. J., and Wier, P. J. (2007). Identification of drug-induced hyper- or hypoprolactinemia in the female rat based on general and reproductive toxicity study parameters. *Birth Defects Res. B Dev. Reprod. Toxicol.* **80,** 253–257.

Roberge, M. T., Hakk, H., and Larsen, G. (2006). Cytosolic and localized inhibition of phosphodiesterase by atrazine in swine tissue homogenates. *Food Chem. Toxicol.* **44,** 885–890.

Sanbuissho, A., Yoshida, M., Hisada, S., Sagami, F., Kudo, S., Kumazawa, T., Ube, M., Komatsu, S., and Ohno, Y. (2009). Collaborative work on evaluation of ovarian toxicity by repeated-dose and fertility studies in female rats. *J. Toxicol. Sci.* **34,** SP1–SP22.

Sanderson, J. T., Boerma, J., Lansbergen, G. W., and van den Berg, M. (2002). Induction and inhibition of aromatase (CYP19) activity by various classes of pesticides in H295R human adrenocortical carcinoma cells. *Toxicol. Appl. Pharmacol.* **182,** 44–54.

Saxena, D., Escamilla-Hernandez, R., Little-Ihrig, L., and Zeleznik, A. J. (2007). Liver receptor homolog-1 and steroidogenic factor-1 have similar actions on rat granulosa cell steroidogenesis. *Endocrinology* **148,** 726–734.

Shibayama, H., Kotera, T., Shinoda, Y., Hanada, T., Kajihara, T., Ueda, M., Tamura, H., Ishihashi, S., and Yamashita, Y. (2009). Collaborative work on evaluation of ovarian toxicity. 14) Two- or four-week repeated-dose studies and fertility study of atrazine in female rats. *J. Toxicol. Sci.* **34,** SP147–SP155.

Stocco, C., Telleria, C., and Gibori, G. (2007). The molecular control of corpus luteum formation, function, and regression. *Endocr. Rev.* **28,** 117–149.

Stocco, C. O., Zhong, L., Sugimoto, Y., Ichikawa, A., Lau, L. F., and Gibori, G. (2000). Prostaglandin F2alpha-induced expression of 20alpha-hydroxysteroid dehydrogenase involves the transcription factor NUR77. *J. Biol. Chem.* **275,** 37202–37211.

Stocco, D. M. (2001). StAR protein and the regulation of steroid hormone biosynthesis. *Annu. Rev. Physiol.* **63,** 193–213.

Stouffer, R. L. (2006). Structure, function, and regulation of the corpus luteum. In *Knobil and Neill's Physiology of Reproduction*, 3rd ed. (J. D. Neill, Ed.), pp. 475–526. Elsevier Academic Press, San Diego, CA.

Suzawa, M., and Ingraham, H. A. (2008). The herbicide atrazine activates endocrine gene networks via non-steroidal NR5A nuclear receptors in fish and mammalian cells. *PLoS One* **3,** e2117.

Taya, K., Mizokawa, T., Matsui, T., and Sasamoto, S. (1983). Induction of superovulation in prepubertal female rats by anterior pituitary transplants. *J. Reprod. Fertil.* **69,** 265–270.

Taya, K., Watanabe, G., and Sasamoto, S. (1985). Radioimmunoassay for progesterone, testosterone, and estradiol-17b using 125I-iodohistamine radioligands. *Jpn. J. Anim. Reprod.* **31,** 186–197.

Telleria, C. M., Parmer, T. G., Zhong, L., Clarke, D. L., Albarracin, C. T., Duan, W. R., Linzer, D. I., and Gibori, G. (1997). The different forms of the prolactin receptor in the rat corpus luteum: developmental expression and hormonal regulation in pregnancy. *Endocrinology* **138,** 4812–4820.

Welsch, F. (2005). The mechanism of ethylene glycol ether reproductive and developmental toxicity and evidence for adverse effects in humans. *Toxicol. Lett.* **156,** 13–28.

Yamada, I., Mizuta, H., Ogawa, K., and Tahara, T. (1990). Comparative pharmacokinetics of sulpiride and N-[(1-butyl-2-pyrrolidinyl)methyl]-2-methyl-5-sulfamoyl-2,3-dihydrobenzofuran-7-carboxamide hydrochloride, a new lipophilic substituted benzamide in rats. *Chem. Pharm. Bull. (Tokyo)* **38,** 2552–2555.

Yoshida, M., Sanbuissyo, A., Hisada, S., Takahashi, M., Ohno, Y., and Nishikawa, A. (2009). Morphological characterization of the ovary under normal cycling in rats and its viewpoints of ovarian toxicity detection. *J. Toxicol. Sci.* **34,** SP189–S197.

Yuan, Y., and Foley, G. (2002). Female reproductive system. In *Handbook of Toxicologic Pathology*, 2nd ed. (W. M. Haschek, C. G. Rousseaux, and M. S. Wallig, Eds.), pp. 847–894. Academic Press, London, UK.

Experimental and Toxicologic Pathology 64 (2012) 775–782

Contents lists available at ScienceDirect

Experimental and Toxicologic Pathology

journal homepage: www.elsevier.de/etp

The newly formed corpora lutea of normal cycling rats exhibit drastic changes in steroidogenic and luteolytic gene expressions

Yoshikazu Taketa[a,b], Midori Yoshida[a,*], Kaoru Inoue[a], Miwa Takahashi[a], Yohei Sakamoto[a], Gen Watanabe[c], Kazuyoshi Taya[c], Jyoji Yamate[b], Akiyoshi Nishikawa[a]

[a] Division of Pathology, National Institute of Health Sciences, 1-18-1 Kamiyoga, Setagaya-ku, Tokyo 158-8501, Japan
[b] Laboratory of Veterinary Pathology, Life and Environmental Sciences, Osaka Prefecture University, 1-58 Rinkuu Ourai Kita, Izumisano, Osaka 598-8531, Japan
[c] Laboratory of Veterinary Physiology, Department of Veterinary Medicine, Faculty of Agriculture, Tokyo University of Agriculture and Technology, 3-5-8 Saiwai-cho, Fuchu, Tokyo 183-8509, Japan

ARTICLE INFO

Article history:
Received 27 July 2010
Accepted 30 January 2011

Keywords:
Corpora lutea
Estrous cycle
Laser microdissection
Progesterone
Rat

ABSTRACT

In normal estrous cycling rats, corpora lutea (CL) regress over several cycles; however, the period during which they secrete progesterone (P4) is strictly limited. In the present study, we clarified the function of CL in normal cycling rats. We especially focused on expression levels of four steroidogenic and two luteolytic genes in the two different populations of the CL (new and old CL) at each estrous stage. The ovaries of female rats at each estrous cycle were collected, and new and old CL were separated with laser microdissection and analyzed for mRNA expression. In the new CL, the expressions of scavenger receptor class B type I (*SR-BI*), steroidogenic acute regulatory protein (*StAR*), and P450 cholesterol side-chain cleavage (*P450scc*) mRNA reached their highest levels at metestrus, and 3β-hydroxysteroid dehydrogenase (*3β-HSD*) mRNA gradually increased from estrus to diestrus. Meanwhile, 20α-hydroxysteroid dehydrogenase (*20α-HSD*) and prostaglandin F2 alpha receptor (*PGF2α-R*) mRNA levels were remarkably low from estrus to metestrus and gradually increased thereafter. These gene levels in new CL corresponded to serum P4 levels during the estrous cycle. In the old CL, all steroidogenic and luteolytic gene levels were consistently high throughout the estrous cycle. These results provide clear evidence that new CL at metestrus have strong steroidogenic activity and through inhibition of luteolysis, maintain P4 production in normal cycling rats. The elevation of 20α-HSD and PGF2α-R levels in new CL at diestrus may be a trigger of functional luteolysis.

1. Introduction

Numerous drugs and chemicals that have been tested in experimental animals have been found to interfere with reproductive function in the female (Yuan and Foley, 2002). These chemicals, which usually target the ovaries, are commonly referred to as ovarian toxicants and frequently cause disturbances in estrous cyclicity in rodents. Other chemicals may act by altering the normal morphology of the reproductive tract (Yoshida et al., 2009). For instance, 4-vinyl-cyclohexene diepoxide (VCD) destroys oocytes and induces the decrease of small follicles (Ito et al., 2009), and ethylene glycol monomethyl ether (EGME) stimulates luteal progesterone (P4) secretion and induces luteal hypertrophy (Dodo et al., 2009). The ovary has two distinct functional components required for estrous cyclicity, the corpora lutea (CL) and the follicles. Understanding the morphology and function of these structures is a prerequisite for understanding the mechanism of ovarian toxicants that disrupt the estrous cycle. The rat estrous cycle is characterized by cyclic variation in P4 levels. There are two discrete periods in the estrous cycle during which P4 is increased. The first occurs in the afternoon of proestrus and the second during the metestrus to diestrus stages (Smith et al., 1975; Tebar et al., 1995). The preovulatory P4 is secreted during proestrus by the Graafian follicles in an luteinizing hormone (LH)-dependent manner. In metestrus and diestrus, secretion is from the CL in an LH-independent manner. The luteal secretion of P4 during the metestrus to diestrus stages begins to rise in the morning of metestrus, reaches peak values by midnight of metestrus, and falls to basal levels thereafter as a result of luteolysis (Kaneko et al., 1986). This drop-off in P4 is considered the beginning of the functional regression of the CL in the normal rat estrous cycle. Additionally, prolactin (PRL) has a crucial role in luteal P4 secretion and structural luteolysis (Stocco et al., 2007).

The P4 biosynthesis in the CL is divided into the following two steps: the uptake, synthesis, and transport of cholesterol, and the processing of cholesterol to P4. Cholesterol is preferentially yielded from circulatory high- and low-density lipoproteins (HDL and LDL);

* Corresponding author. Tel.: +81 3 3700 9821; fax: +81 3 3700 1425.
E-mail address: midoriy@nihs.go.jp (M. Yoshida).

0940-2993/$ – see front matter © 2011 Elsevier GmbH. All rights reserved.
doi:10.1016/j.etp.2011.01.015

and HDL is the main source of cholesterol for CL in rodents (Bruot et al., 1982; Schuler et al., 1981). Scavenger receptor class B type I (SR-BI) is now considered as the authentic HDL receptor mediating the selective uptake of HDL-derived cholesterol ester (Acton et al., 1996). After uptake, the cholesterol esters are transported to the outer mitochondrial membrane and then to the inner membrane by several proteins including steroidogenic acute regulatory protein (StAR) (Stocco et al., 2001). Once cholesterol reaches the inner mitochondrial membrane, its transformation into P4 begins. In this step, mitochondrial P450 cholesterol side-chain cleavage (P450scc) (Oonk et al., 1989) and 3β-hydroxysteroid dehydrogenase (3β-HSD) which are located in the smooth endoplasmic reticulum (Peng et al., 2002) play principal roles.

The P4 secretion from the CL in rodents is regulated by the balance between synthesis and catabolism. Briefly, it depends not only on the amount of P4 synthesized by the luteal cells but also on the expression of the enzyme 20α-hydroxysteroid dehydrogenase (20α-HSD) that catabolizes P4 into the inactive progestin, 20α-dihydroprogesterone (20α-DHP). Once 20α-HSD becomes expressed in the CL, P4 secretion declines and 20α-DHP becomes the major steroid secreted by luteal cells (Stocco et al., 2000).

In rodents, the decrease in P4 is an index of the functional regression of the CL. The structural regression occurs after the initial decline in P4 output and is morphologically observed as luteal cell apoptosis (Stocco et al., 2007). In the functional regression, several factors including prostaglandin F2 alpha (PGF2α) and LH have been implicated in the downregulation of luteal P4 production (Pharriss and Wyngarden, 1969; Plas-Roser et al., 1988). Meanwhile, several signals including PRL, PGF2α, tumor necrosis factor-alpha (TNFα), and Fas ligand (FasL) have been indicated in the induction of cell death required for the structural regression of the CL (Gaytan et al., 2000; Roughton et al., 1999; Stocco et al., 2007; Yadav et al., 2005).

There are two main types of CL: those which are newly formed by the current ovulation (new CL) and CL remaining from prior estrous cycles (old CL) (Bowen and Keyes, 2000). New and old CL are morphologically distinguishable at each estrous stage, and new CL drastically change their morphology during the estrous cycle (Yoshida et al., 2009).

As mentioned above, the CL in cycling rats secrete P4 for a limited period prior to undergoing functional luteolysis a few days after being formed. It is likely that both new and old CL are essential to estrous cycle regulation. Therefore, it is important to analyze normal functional changes of steroidogenesis in each type of CL across the estrous cycle in order to understand how they may be affected by ovarian toxicants. The expression of steroidogenic and luteolytic factors across the estrous cycle has been partially elucidated (Peluffo et al., 2006; Slot et al., 2006; Takahashi et al., 1995); however, little is known about the transitions in gene expression that occur in new and old CL across the estrous cycle. In the present study, we investigated the transitions in luteal gene expression and steroidogenesis in each rat estrous stage to identify the potential targets of ovarian toxicants. We separated new CL from old CL using laser microdissection (LMD). We focused on four steroidogenic genes: *SR-BI*, *StAR*, *P450scc*, and *3β-HSD*, and two luteolytic genes: *20α-HSD* and PGF2α receptor (*PGF2α-R*). Additionally, immunohistochemical features of P450scc and 3β-HSD in both types of CL were also examined.

2. Materials and methods

2.1. Animals

Female 6-week-old Sprague–Dawley (Crl:CD) rats were purchased from Charles River Laboratories Japan, Inc. (Yokohama, Japan). They were housed in plastic cages (3 or 4 animals/cage) maintained at 23–25 °C and a relative humidity of 50–60% with a 12-h light cycle. Commercial rodent chow (CRF-1; Oriental Yeast Co., Ltd., Tokyo, Japan) and drinking water were available *ad libitum* throughout the experiment. The animal protocols were reviewed and approved by the Animal Care and Use Committee of the National Institute of Health Sciences, Japan.

Estrous cyclicity was monitored by daily vaginal smears. When the rats reached 10 weeks of age, they were euthanized by decapitation at each of the estrous stages (estrus, metestrus, diestrus, and proestrus: 6–7 rats per group) between 10:00 and 12:00 AM. These estrous stages were also confirmed by microscopic examination of the vagina and uterus. For LMD, the left ovaries were rapidly removed, embedded in OCT compound, and frozen with liquid nitrogen. The right ovaries were fixed in 4% paraformaldehyde for one day, and routinely processed with hematoxylin and eosin (HE) and immunohistochemical stains.

2.2. Laser microdissection of new or old corpora lutea in each estrous stage

The OCT-embedded frozen ovaries were sectioned into 10 μm slices onto membrane-based laser microdissection slides (Leica Microsystems, Wetzlar, Germany) and fixed in 70% ethanol for 1 min. The sections were then hydrated in diethylpyrocarbonate (DEPC)-treated water for 10 s, stained with toluidine blue for 30 s, washed in DEPC water for 30 s, dehydrated by dipping sequentially in 70, 95, and 100% ethanol and then air dried. New CL (CL which are newly formed by the current ovulation) and old CL (CL remaining from prior estrous cycles) were visualized and captured using a Leica LMD6000 laser microdissection system (Leica Microsystems) (Sakurada et al., 2006).

2.3. Extraction of total RNA and reverse transcription

Laser-captured tissues were pooled in lysis buffer and RNA was extracted with the RNeasy Mini kit (Qiagen, Valencia, CA, USA) according to the manufacturer's instructions. Residual genomic DNA was removed by an on-column RNase-free DNase Set (Qiagen) during RNA purification. The RNA was then precipitated with 14 μl ddH_2O, checked for concentration and purity using the spectrophotometer (NanoDrop ND-1000, Thermo Fischer Scientific Inc., Waltham, MA, USA), and stored at −80 °C until analysis. For cDNA synthesis, reverse transcription (RT) was performed with the Sensiscript RT Kit (Qiagen) using random primers in a 20 μl final volume following the manufacturer's instructions.

2.4. Real-time quantitative PCR

Messenger RNA levels were analyzed using an ABI Prism 7900 Sequence Detection System and TaqMan® gene expression assays (Applied Biosystems, Foster City, CA, USA) for *SR-BI*, *StAR*, *P450scc*, *3β-HSD*, *20α-HSD*, *PGF2α-R*, and hypoxanthine-guanine phosphoribosyltransferase (*HPRT*) (Table 1). The PCR cycling conditions included an initial denaturation at 95 °C for 20 s followed by 50 cycles at 95 °C for 1 s and 60 °C for 20 s. To compare mRNA levels among samples, mRNA for each gene of interest was normalized to the expression of a housekeeping gene, *HPRT*, using the standard curve method. Real-time PCR reactions were performed with the Universal TaqMan 2× Fast Universal PCR Master Mix (Applied Biosystems) in a 20 μl reaction volume.

2.5. Immunohistochemistry

The right ovarian sections were deparaffinized, treated with 90% methanol containing 3% H_2O_2 for 10 min at room tempera-

Table 1
Primers and probes used for real-time PCR analysis.

Gene	Primer and probe		GenBank accession No.
SR-BI	Forward	5′-CCGAATCCTCACTGGAATTCTTC-3′	NM_031541
	Reverse	5′-CGAACACCCTTGATTCCTGGTA-3′	
	Probe	5′-VIC-AAGCCTGCAGATCTATGA-MGB-3′	
StAR	Forward	5′-GGGAGAGTGGAACCCAAATGT-3′	NM_031558
	Reverse	5′-CATGGGTGATGACTGTGTCTTTTC-3′	
	Probe	5′-VIC-AAGGAAATCAAGGTCCTGAAG-MGB-3′	
P450scc	Forward	5′-TCTCCTCTACCAACAGTCCTCGAT-3′	BC089100
	Reverse	5′-TGGTACAGGTTTATCCAACCATTG-3′	
	Probe	5′-VIC-CTTCAATGAGATCCCTTC-MGB-3′	
3β-HSD	Forward	5′-GCCCAACTCCTACAAGAAGATCAT-3′	L17138
	Reverse	5′-CTCGGCCATCTTTTTGCTGTATG-3′	
	Probe	5′-VIC-ATGTGCTTTCATGATGCTCT-MGB-3′	
20α-HSD	Forward	5′-TTTCAATGAGGAGAGAATCAGAGAGA-3′	L32601
	Reverse	5′-CCATGTCATCTGAAGCCAACTG-3′	
	Probe	5′-VIC-CCTGCAGGTCTTTGAT-MGB-3′	
PGF2α-R	Forward	5′-CTCTGGCTTGTGCCCACTTT-3′	U47287
	Reverse	5′-CCGATGCACCTCTCAATGG-3′	
	Probe	5′-VIC-CCTGGGCAGTACGATG-MGB-3′	
HPRT	Forward	5′-GCCGACCGGTTCTGTCAT-3′	X62085
	Reverse	5′-GGTCATAACCTGGTTCATCATCAC-3′	
	Probe	5′-FAM-CAGTCCCAGCGTCGTG-TAMRA-3′	

ture (RT), and washed twice in PBS. For P450scc immunostaining, sections were heated in a citric acid buffer 0.01 M (pH = 7.0) at 95 °C for 5 min and washed twice in PBS. For 3β-HSD immunostaining, there was no antigen retrieval treatment. A blocking solution was then applied for 30 min. The blocking solutions were 3% goat serum in PBS for P450scc and 3% rabbit serum in PBS for 3β-HSD. Sections were then incubated overnight with P450scc antibody (1:200; Millipore Corporation, Temecula, CA, USA) or 3β-HSD antibody (1:200; Santa Cruz, CA, USA) at 4 °C. After washing 4 times in PBS, the sections were then incubated with the secondary antibody (HISTOFINE SIMPLESTAIN MAX-PO, Nichirei Bioscience, Tokyo, Japan) matched to the primary antibody for 30 min at RT. The reaction products were visualized with 3,3′-diaminobenzidine (DAB, Dojindo Laboratories, Kumamoto, Japan). The sections were counterstained with Mayer's hematoxylin. To test the specificity of immunostaining, negative controls were run without the primary antibodies.

2.6. Hormone assays

Serum samples obtained after decapitation were stored at −80 °C until assay. The serum concentrations of follicle-stimulating hormone (FSH), LH, inhibin-α (INH), PRL, estradiol-17β (E_2), and P4 were determined using double-antibody radioimmunoassay and ^{125}I-labeled radioligands. National Institute of Diabetes and Digestive and Kidney Disease (NIDDK) radioimmunoassay kits were employed for rat FSH, LH, and PRL (NIAMDD, NIH, Bethesda, MD, USA) as described by Taya et al. (1983). Immunoreactive INH in the serum was analyzed using a rabbit anti-serum, TNDH-1 (Hamada et al., 1989). The serum concentrations of E_2 and P4 were also measured as described by Taya et al. (1985).

2.7. Statistical analysis

Hormonal data are presented as the mean ± SEM. Real-time PCR data are presented as the mean ± SD. Variances in data of hormone concentrations and relative mRNA levels of new and old CL across the estrous cycle were checked for homogeneity by Bartlett's procedure. If the variance was homogeneous, the data were assessed by one-way ANOVA. If not, the Kruskal–Wallis test was applied. When statistically significant differences were indicated, the Dunnett's multiple test was employed. Differences of mRNA level between new and old CL for each estrous stage were evaluated by Welch's *t*-test. $P < 0.05$ was considered statistically significant.

3. Results

3.1. Changes of serum hormone levels during the estrous cycle

The serum P4 and LH levels were significantly higher at metestrus, and the E_2 level was gradually elevated from estrus to proestrus (Fig. 1). The concentrations of PRL, FSH, and INH were not significantly different across the estrous cycle (Fig. 1).

3.2. Expressions of steroidogenic and luteolytic genes in new and old CL during the estrous cycle

The changes in mRNA expression for each estrous stage in new and old CL are shown in Figs. 2 and 3. In the new CL, the levels of *SR-BI*, *StAR* and *P450scc* mRNA reached their highest values at metestrus and gradually decreased thereafter (*SR-BI*; 544, 228, and 113%, *StAR*; 596, 407, and 325%, *P450scc*; 231, 146, and 68% at metestrus, diestrus, and proestrus, respectively, compared to estrus) (Fig. 2A–C). There were no differences in the levels of these genes in old CL throughout the estrous cycle (Fig. 2A–C). The expression of *3β-HSD* mRNA was gradually increased from estrus to diestrus in new CL, but decreased at proestrus (155, 172, and 121% at metestrus, diestrus, and proestrus, respectively, compared to estrus) (Fig. 2D). *3β-HSD* mRNA expression in old CL showed a similar change, though to a consistently lesser degree (Fig. 2D). In the new CL, *20α-HSD* and *PGF2α-R* mRNA levels were extremely low at estrus and metestrus, and drastically increased from diestrus to proestrus (*20α-HSD*; 92, 4587, and 10,755%, *PGF2α-R*; 429, 3363, and 6784% at metestrus, diestrus, and proestrus, respectively, compared to estrus) (Fig. 3A and B). In the old CL, expression of these genes was higher at baseline (Fig. 3A and B).

There were differences in mRNA levels between new and old CL. The expression of *SR-BI* mRNA was significantly higher in new CL than in old CL at metestrus. The reverse was observed at estrus and proestrus (Fig. 2A). *StAR* mRNA expression tended to be higher in old CL than in new CL throughout the estrous cycle, and was significantly higher at estrus, diestrus, and proestrus stages (Fig. 2B). *P450scc* and *3β-HSD* mRNA levels had similar patterns, both of them being significantly higher in new CL than in old CL at metestrus, although there were no differences at the other estrous

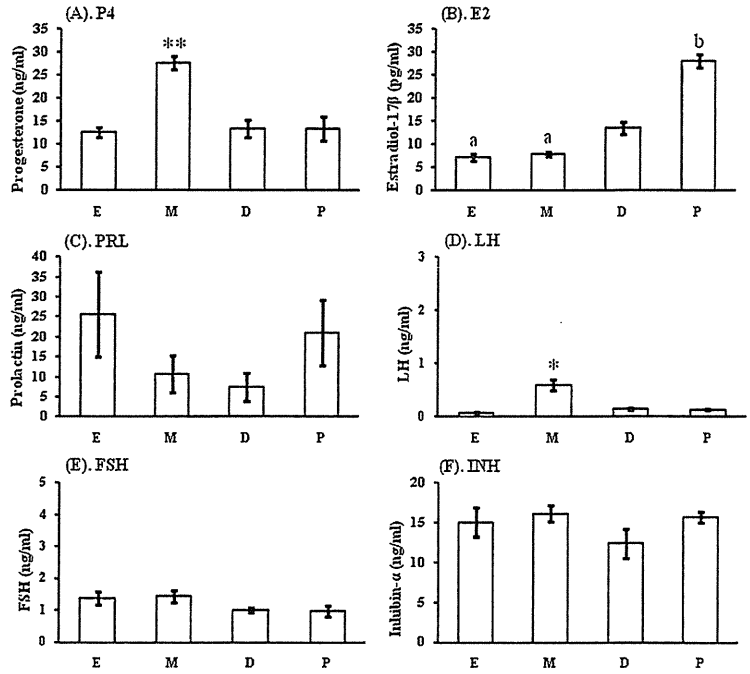

Fig. 1. Serum hormone levels at each estrous cycle stage. Data represent serum P4 (A), E_2 (B), PRL (C), LH (D), FSH (E), and INH (F) levels (mean ± SEM) at each estrous stage (E: estrus; M: metestrus; D: diestrus; P: proestrus). Six to seven animals were examined ($n = 6–7$). Double asterisks ($P < 0.01$), asterisk ($P < 0.05$) and letters ($P < 0.01$) indicate significant differences.

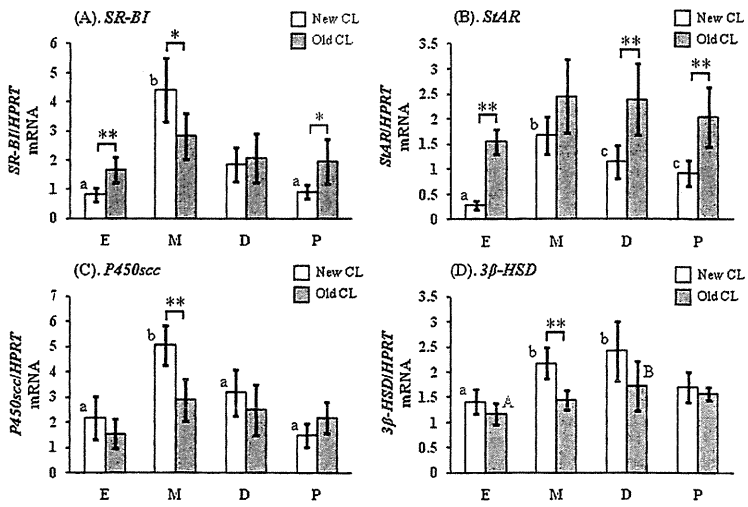

Fig. 2. The mRNA levels of steroidogenic factors in new and old CL across the estrous cycle. Relative mRNA levels of *SR-BI* (A), *StAR* (B), *P450scc* (C), and 3β-*HSD* (D) were presented at each estrous stage (E: estrus; M: metestrus; D: diestrus; P: proestrus). Five animals were examined. Data were normalized for *HPRT* mRNA levels in each sample and presented as the mean ± SD, with asterisks and letters indicating significant differences (**$P < 0.01$; *$P < 0.05$; letters $P < 0.05$).

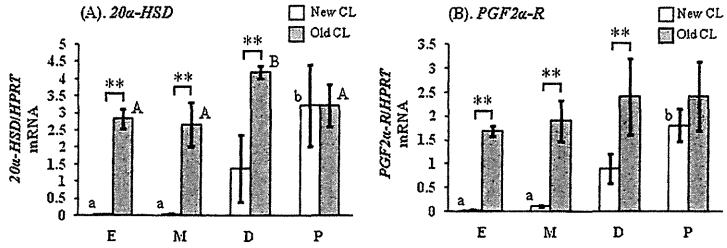

Fig. 3. The mRNA levels of luteolytic factors in new and old CL across the estrous cycle. Relative mRNA levels of 20α-*HSD* (A) and *PGF2α-R* (B) were presented at each estrous stage (E: estrus; M: metestrus; D: diestrus; P: proestrus). Five animals were examined. Data were normalized for *HPRT* mRNA levels in each sample and presented as the mean ± SD, with asterisks and letters indicating significant differences (**$P < 0.01$; different letters $P < 0.05$).

stages (Fig. 2C and D). 20α-*HSD* and *PGF2α-R* mRNA levels also had similar patterns, but those were much lower in new CL than in old CL at estrus, metestrus, and diestrus stages (Fig. 3A and B). Thus, 20α-*HSD* and *PGF2α-R* mRNA levels were drastically different between new and old CL.

3.3. Immunohistochemical examination of P450scc and 3β-HSD in new and old CL across the estrous cycle

The P450scc- and 3β-HSD-positive luteal cells were observed in all CL throughout the estrous cycle (Figs. 4 and 5). In new CL, the P450scc immunostaining intensity was weak at estrus, but was intensely expressed at the other estrous stages (metestrus, diestrus, and proestrus) (Fig. 4a, c, e, and g). The luteal cells of new CL at metestrus, diestrus, and proestrus stages were strongly and uniformly stained (Fig. 4a, c, e, and g). In contrast, the P450scc-positive luteal cells were observed throughout the estrous cycle in old CL (Fig. 4b, d, f, and h). P450scc strongly positive luteal cells were decreased and scattered in old CL at all stages (Fig. 4b, d, f, and h), and the staining intensities gradually weakened as the CL aged. The profiles of 3β-HSD-positive luteal cells were quite similar to those of P450scc, with the exception of being somewhat weaker (Fig. 5).

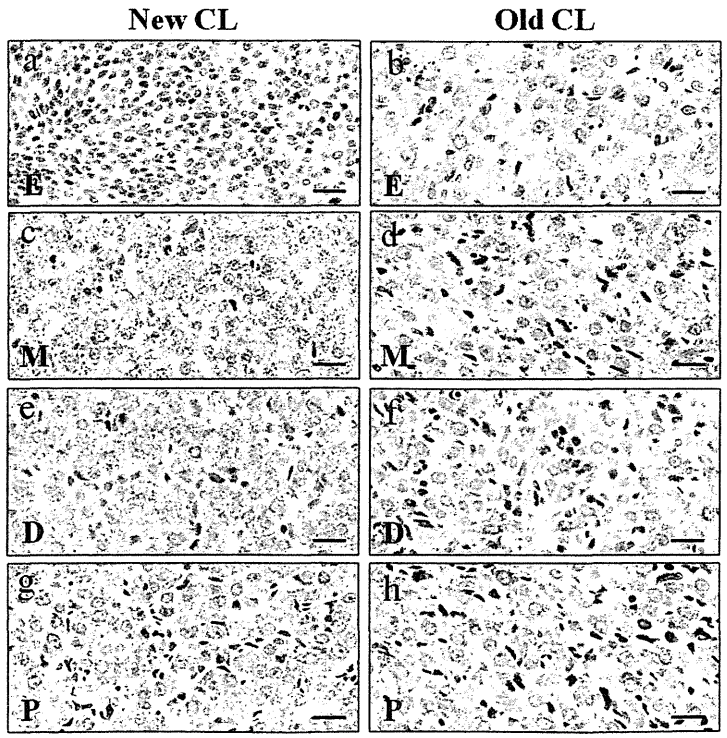

Fig. 4. Immunohistochemistry of P450scc in the cycling rat CL. The left-side pictures (a, c, e, and g) represent new CL, and right-side ones (b, d, f, and h) represent old CL at each estrous stage (E: estrus; M: metestrus; D: diestrus; P: proestrus). Bars indicate 20 μm.

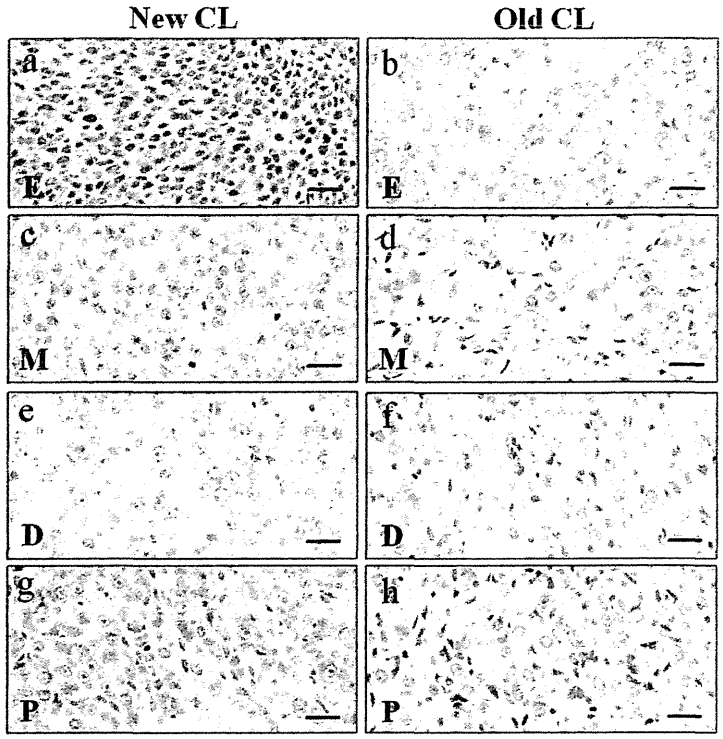

Fig. 5. Immunohistochemistry of 3β-HSD in the cycling rat CL. The left-side pictures (a, c, e, and g) represent new CL, and right-side ones (b, d, f, and h) represent old CL at each estrous stage (E: estrus; M: metestrus; D: diestrus; P: proestrus). Bars indicate 20 μm.

4. Discussion

This study investigated the transition of steroidogenic and luteolytic gene levels in new and old CL in normal cycling rats using the LMD method. Our results demonstrated drastic changes in the gene expression in new CL across the estrous cycle. In the hormone analysis, a significantly higher level of serum P4 in the forenoon at metestrus and the gradual elevation in the E_2 level from estrus to proestrus were consistent with prior reports (Kaneko et al., 1986; Smith et al., 1975; Watanabe et al., 1990). The elevation of LH at metestrus gyrated within the background range. It confirmed that the serum P4 elevation at metestrus was independent of other hormone levels.

In accordance with elevation of serum P4, the steroidogenic genes, *SR-BI*, *StAR*, and *P450scc* mRNA expression peaked at metestrus in new CL then gradually declined. In contrast, those of old CL remained somewhat elevated, making these three steroidogenic genes useful markers for P4 production in new CL. Li et al. (1998) reported that the expression of *SR-BI* mRNA remarkably increased with the completion of luteinization in rats. The reason for this discrepancy remains unclear, but may be explained by differences in experimental conditions. In the previous report, the experimental model employed immature rats treated with equine chronic gonadotropin (eCG) and human chorionic gonadotropin (hCG), whereas mature intact cycling rats were used in the present study.

The present study showed no significant differences in the *P450scc* and 3β-*HSD* mRNA levels between new and old CL except at metestrus. *StAR* mRNA expression in old CL was consistently higher than that in new CL throughout the estrous cycle. This suggests an increased capacity for steroidogenesis in luteal cells of old CL compared to those in new CL. In the present study, the immunohistochemical expression of P450scc did not correspond to mRNA expression. P450scc-positive cells were observed in all CL throughout the estrous cycle. Although the mRNA level was relatively high throughout the estrous cycle, immunohistochemical staining was very slight at estrus in new CL. It is plausible that new CL at estrus may lack the functional maturity required to express P450scc protein. The P450scc staining intensity was gradually weakened as the CL aged. This weak intensity may be attributed to increased interstitial cells in the regressing old CL.

The immunohistochemical expression of 3β-HSD also failed to parallel its mRNA expression. A relatively high level of mRNA was present in all CL throughout the estrous cycle; however, only slight immunoreactivity was present at estrus in new CL. The weak reactions were also considered a reflection of the immaturity of new CL at estrus. The 3β-HSD staining intensity was also gradually weakened as the CL aged, and this again may have been due to the increased interstitial cells in the regressing old CL. Unlike the other steroidogenic factors, the expression of 3β-*HSD* mRNA in new CL was consistently high until diestrus in the present study. In immature rats treated with eCG and hCG, luteal 3β-

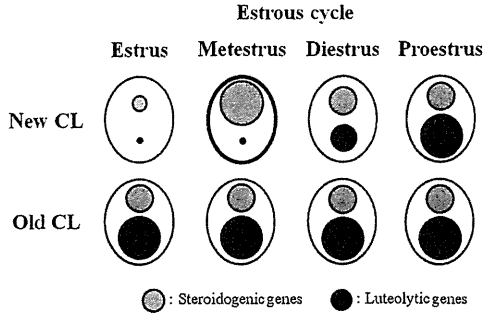

Fig. 6. Overview of steroidogenic and luteolytic gene levels in new and old CL across the estrous cycle in rats. The sizes of the circles represent the levels of steroidogenic genes (gray circles) and luteolytic genes (black circles). The new CL at metestrus, which have the capacity for P4 secretion, showed notably high steroidogenic gene and low luteolytic gene levels. Luteolytic genes in new CL were remarkably low at estrus and metestrus, and gradually increased thereafter. In the old CL, relatively high steroidogenic and markedly high luteolytic gene levels were consistently retained throughout the estrous cycle.

HSD mRNA expression is drastically increased as the CL is formed, with expression sustained throughout the pseudopregnant state (Kaynard et al., 1992). It is suggested that the 3β-HSD expression has a high threshold level of down-regulation by luteolytic factors including PGF2α at diestrus, which is the first stage of functional regression.

The luteolytic genes in new CL showed drastic changes across the estrous cycle ranging from extremely low from estrus to metestrus with a gradual increase thereafter. The transition of 20α-*HSD* mRNA was similar to that of *PGF2α-R*, consistent with 20α-*HSD* mRNA being upregulated by PGF2α. The elevations of 20α-*HSD* and *PGF2α-R* mRNA caused functional luteolysis at diestrus in new CL. The functional luteolysis of new CL starts at diestrus (Sugino and Okuda, 2007). PGF2α plays a crucial role in this process. Administration of PGF2α induces a drop in levels of circulating P4 in rodents (Pharriss and Wyngarden, 1969). In rodents, this reduction of luteal P4 secretion by PGF2α is not the result of decreased synthesis of P4, but rather due to the metabolism of P4 to 20α-DHP (Stocco et al., 2007). PGF2α stimulates the expression of the 20α-*HSD* gene and the activity of this enzyme (Stocco, 2001; Strauss and Stambaugh, 1974) by inducing the expression of the nuclear orphan receptor and transcription factor Nur77, which leads to the transcriptional stimulation of 20α-HSD in the CL (Stocco et al., 2000). The circulating level of 20α-DHP throughout the estrous cycle was previously reported (Nequin et al., 1979), which showed low level during metestrus to diestrus and high level during proestrus to estrus. It seemed that the elevation of 20α-DHP level during proestrus to estrus was attributed to the functionally regressed new CL from diestrus.

An overview of luteal gene expression during the estrous cycle is presented in Fig. 6. The present study found a drastic change in luteal function across the estrous cycle. Our results indicate that both high expression of steroidogenic genes and low expression of luteolytic genes are required for P4 secretion in newly formed CL in a normal estrous cycle. The elevation of luteolytic factors, 20α-HSD and PGF2α-R, plays an important role in the drop of P4 production. Additionally, old CL seemed to have steroidogenic function throughout the estrous cycle, but the P4 produced by them was invariably converted into inactive 20α-DHP by 20α-HSD.

To our knowledge, our study is the first report demonstrating the changes in steroidogenic and luteolytic gene expressions in new and old CL during the estrous cycle with the LMD method. The present study demonstrated that LMD is a useful tool to link the structural and functional changes of each component in the ovary including the CL and follicles. In addition, the results in the present study indicate that consideration of the functional and structural changes in the CL is very important for detecting ovarian toxicants targeting CL, and the changes of steroidogenic and luteolytic gene levels may have a crucial role in onset of lutel toxicity. However, as our study mainly focused on gene expression, additional studies are needed to document these changes on the protein level.

Acknowledgments

We thank Ms. Tomomi Morikawa, Ms. Ayako Kaneko, and Ms. Yoshimi Komatsu for their excellent technical assistance. We also appreciate Dr. Satoru Hosokawa and Dr. Akira Inomata (Drug Safety Japan, Global Drug Safety, Biopharmaceutical Assessments Core Function Unit, Eisai Product Creation Systems, Eisai Co., Ltd.) for their helpful suggestions. This study was supported by Health and Labour Sciences Research Grants, Research on Risk of Chemical Substances, Ministry of Health, Labour and Welfare [H22-Toxicol-003].

References

Acton S, Rigotti A, Landschulz KT, Xu S, Hobbs HH, Krieger M. Identification of scavenger receptor SR-BI as a high density lipoprotein receptor. Science 1996;271:518–20.

Bowen JM, Keyes PL. Repeated exposure to prolactin is required to induce luteal regression in the hypophysectomized rat. Biol Reprod 2000;63:1179–84.

Bruot BC, Wiest WG, Collins DC. Effect of low density and high density lipoproteins on progesterone secretion by dispersed corpora luteal cells from rats treated with aminopyrazolo-(3,4-d)pyrimidine. Endocrinology 1982;110:1572–8.

Dodo T, Taketa Y, Sugiyama M, Inomata A, Sonoda J, Okuda Y, et al. Collaborative work on evaluation of ovarian toxicity. (11) Two- or four-week repeated-dose studies and fertility study of ethylene glycol monomethyl ether in female rats. J Toxicol Sci 2009;34(Suppl. 1):SP121–8.

Gaytan F, Morales C, Bellido C, Aguilar R, Millan Y, Martin De Las Mulas J, et al. Progesterone on an oestrogen background enhances prolactin-induced apoptosis in regressing corpora lutea in the cyclic rat: possible involvement of luteal endothelial cell progesterone receptors. J Endocrinol 2000;165:715–24.

Hamada T, Watanabe G, Kokuho T, Taya K, Sasamoto S, Hasegawa Y, et al. Radioimmunoassay of inhibin in various mammals. J Endocrinol 1989;122:697–704.

Ito A, Mafune N, Kimura T. Collaborative work on evaluation of ovarian toxicity. (4) Two- or four-week repeated dose study of 4-vinylcyclohexene diepoxide in female rats. J Toxicol Sci 2009;34(Suppl. 1):SP53–8.

Kaneko S, Sato N, Sato K, Hashimoto I. Changes in plasma progesterone, estradiol, follicle-stimulating hormone and luteinizing hormone during diestrus and ovulation in rats with 5-day estrous cycles: effect of antibody against progesterone. Biol Reprod 1986;34:488–94.

Kaynard AH, Periman LM, Simard J, Melner MH. Ovarian 3 beta-hydroxysteroid dehydrogenase and sulfated glycoprotein-2 gene expression are differentially regulated by the induction of ovulation, pseudopregnancy, and luteolysis in the immature rat. Endocrinology 1992;130:2192–200.

Li X, Peegel H, Menon KM. In situ hybridization of high density lipoprotein (scavenger, type 1) receptor messenger ribonucleic acid (mRNA) during folliculogenesis and luteinization: evidence for mRNA expression and induction by human chorionic gonadotropin specifically in cell types that use cholesterol for steroidogenesis. Endocrinology 1998;139:3043–9.

Nequin LG, Alvarez J, Schwartz NB. Measurement of serum steroid and gonadotropin levels and uterine and ovarian variables throughout 4 day and 5 day estrous cycles in the rat. Biol Reprod 1979;20:659–70.

Oonk RB, Krasnow JS, Beattie WG, Richards JS. Cyclic AMP-dependent and -independent regulation of cholesterol side chain cleavage cytochrome P-450 (P-450scc) in rat ovarian granulosa cells and corpora lutea. cDNA and deduced amino acid sequence of rat P-450scc. J Biol Chem 1989;264:21934–42.

Peluffo MC, Bussmann L, Stouffer RL, Tesone M. Expression of caspase-2, -3, -8 and -9 proteins and enzyme activity in the corpus luteum of the rat at different stages during the natural estrous cycle. Reproduction 2006;132:465–75.

Peng L, Arensburg J, Orly J, Payne AH. The murine 3beta-hydroxysteroid dehydrogenase (3beta-HSD) gene family: a postulated role for 3beta-HSD VI during early pregnancy. Mol Cell Endocrinol 2002;187:213–21.

Pharriss BB, Wyngarden LJ. The effect of prostaglandin F 2alpha on the progestogen content of ovaries from pseudopregnant rats. Proc Soc Exp Biol Med 1969;130:92–4.

Plas-Roser S, Muller B, Aron C. Estradiol involvement in the luteolytic action of LH during the estrous cycle in the rat. Exp Clin Endocrinol 1988;92:145–53.

Roughton SA, Lareu RR, Bittles AH, Dharmarajan AM. Fas and Fas ligand messenger ribonucleic acid and protein expression in the rat corpus luteum during apoptosis-mediated luteolysis. Biol Reprod 1999;60:797–804.

Sakurada Y, Shirota M, Inoue K, Uchida N, Shirota K. New approach to in situ quantification of ovarian gene expression in rat using a laser microdissection technique: relationship between follicle types and regulation of inhibin-alpha and cytochrome P450 aromatase genes in the rat ovary. Histochem Cell Biol 2006;126:735–41.

Schuler LA, Langenberg KK, Gwynne JT, Strauss 3rd JF. High density lipoprotein utilization by dispersed rat luteal cells. Biochim Biophys Acta 1981;664:583–601.

Slot KA, Voorendt M, de Boer-Brouwer M, van Vugt HH, Teerds KJ. Estrous cycle dependent changes in expression and distribution of Fas, Fas ligand, Bcl-2, Bax, and pro- and active caspase-3 in the rat ovary. J Endocrinol 2006;188:179–92.

Smith MS, Freeman ME, Neill JD. The control of progesterone secretion during the estrous cycle and early pseudopregnancy in the rat: prolactin, gonadotropin and steroid levels associated with rescue of the corpus luteum of pseudopregnancy. Endocrinology 1975;96:219–26.

Stocco C, Callegari E, Gibori G. Opposite effect of prolactin and prostaglandin F(2 alpha) on the expression of luteal genes as revealed by rat cDNA expression array. Endocrinology 2001;142:4158–61.

Stocco C, Telleria C, Gibori G. The molecular control of corpus luteum formation, function, and regression. Endocr Rev 2007;28:117–49.

Stocco CO, Zhong L, Sugimoto Y, Ichikawa A, Lau LF, Gibori G. Prostaglandin F2alpha-induced expression of 20alpha-hydroxysteroid dehydrogenase involves the transcription factor NUR77. J Biol Chem 2000;275:37202–11.

Stocco DM. StAR protein and the regulation of steroid hormone biosynthesis. Annu Rev Physiol 2001;63:193–213.

Strauss 3rd JF, Stambaugh RL. Induction of 20 alpha-hydroxysteroid dehydrogenase in rat corpora lutea of pregnancy by prostaglandin F-2 alpha. Prostaglandins 1974;5:73–85.

Sugino N, Okuda K. Species-related differences in the mechanism of apoptosis during structural luteolysis. J Reprod Dev 2007;53:977–86.

Takahashi M, Iwata N, Hara S, Mukai T, Takayama M, Endo T. Cyclic change in 3 alpha-hydroxysteroid dehydrogenase in rat ovary during the estrous cycle. Biol Reprod 1995;53:1265–70.

Taya K, Mizokawa T, Matsui T, Sasamoto S. Induction of superovulation in prepubertal female rats by anterior pituitary transplants. J Reprod Fertil 1983;69:265–70.

Taya K, Watanabe G, Sasamoto S. Radioimmunoassay for progesterone, testosterone, and estradiol-17β using 125I-iodohistamine radioligands. Jpn J Anim Reprod 1985;31:186–97.

Tebar M, Ruiz A, Gaytan F, Sanchez-Criado JE. Follicular and luteal progesterone play different roles synchronizing pituitary and ovarian events in the 4-day cyclic rat. Biol Reprod 1995;53:1183–9.

Watanabe G, Taya K, Sasamoto S. Dynamics of ovarian inhibin secretion during the oestrous cycle of the rat. J Endocrinol 1990;126:151–7.

Yadav VK, Lakshmi G, Medhamurthy R. Prostaglandin F2alpha-mediated activation of apoptotic signaling cascades in the corpus luteum during apoptosis: involvement of caspase-activated DNase. J Biol Chem 2005;280:10357–67.

Yoshida M, Sanbuissyo A, Hisada S, Takahashi M, Ohno Y, Nishikawa A. Morphological characterization of the ovary under normal cycling in rats and its viewpoints of ovarian toxicity detection. J Toxicol Sci 2009;34(Suppl. 1):SP189–97.

Yuan Y, Foley G. Female reproductive system. In: Haschek WM, Rousseaux CG, Wallig MS, editors. Handbook of toxicologic pathology. 2nd ed. London: Academic Press; 2002. p. 847–94.

Cancer Science
The official journal of the Japanese Cancer Association JCA

Development of an early induction model of medulloblastoma in Ptch1 heterozygous mice initiated with *N*-ethyl-*N*-nitrosourea

Miwa Takahashi,[1,4] Saori Matsuo,[1,2] Kaoru Inoue,[1] Kei Tamura,[1] Kaoru Irie,[1] Yukio Kodama[3] and Midori Yoshida[1]

[1]Division of Pathology, National Institute of Health Sciences, Setagaya-ku, Tokyo; [2]Pathogenetic Veterinary Science, United Graduate School of Veterinary Sciences, Gifu University, Gifu; [3]Division of Toxicology, National Institute of Health Sciences, Setagaya-ku, Tokyo, Japan

(Received June 1, 2012/Revised August 1, 2012/Accepted August 22, 2012/Accepted manuscript online August 31, 2012/Artide first published online October 30, 2012)

Mice heterozygous for the *ptch1* gene (ptch1 mice) are known as a valuable model of medulloblastoma, a common brain tumor in children. To increase the incidence and reduce the time required for tumor development, allowing for evaluation of modifier effects on medulloblastoma in a short time, we attempted to develop an early induction model of medulloblastoma in ptch1 mice initiated with *N*-ethyl-*N*-nitrosourea (ENU). Ptch1 mice and their wild-type littermates received a single intraperitoneal injection of ENU (10, 50 or 100 mg/kg) on postnatal day 1 (d1) or 4 (d4), and histopathological assessment of brains was conducted at 12 weeks of age. The width of the external granular layer (EGL), a possible origin of medulloblastoma, after injection of 100 mg ENU on d1 or d4 was measured in up to 21-day-old mice. Cerebellar size was apparently reduced at the 50 mg dose and higher regardless of genotype. Microscopically, early lesions of medulloblastomas occurred with a high incidence only in ptch1 mice receiving 10 mg on d1 or d4, but a significant increase was not observed in other groups. Persistent EGL cells and misalignment of Purkinje cells were increased dose-dependently. Although EGL was strikingly decreased after ENU injection, strong recovery was observed in mice of the d1-treated group. In summary, neonatal treatment with ENU is available for the induction of medulloblastoma in ptch1 mice, and 10 mg of ENU administered on d1 appeared to be an appropriate dose to induce medulloblastoma. (*Cancer Sci* 2012; 103: 2051–2055)

Medulloblastoma, a primitive neuroectodermal tumor that develops in the cerebellum, is the most common brain tumor of childhood.[1] The etiology of childhood brain tumors remains largely unknown, but previous studies have suggested associations between childhood brain tumors and chemicals such as pesticides and nitrates.[2–4] These studies are mainly epidemiological, and there are few investigations into the effects of chemical exposure during development on childhood tumor using animal models.

Recent genomic approaches have demonstrated the existence of four distinct subtypes with demographic, transcriptional profiles and clinical outcome.[5,6] In these subtypes, the tumors with activation of the Sonic hedgehog (Shh)-Ptch signaling pathway belong to the SHH group, and are considered to arise from granule cell precursors (GCPs) in the external granular layer (EGL) of the developing cerebellum.[7] Since Shh signaling is known to drive proliferation in the GCPs, it has been suggested that the pathway dysregulation resulting from genomic alterations of its components presumably drives medulloblastoma formation.[7]

Mice heterozygous for the *ptch1* gene (ptch1 mice) are an important model for medulloblastoma. Homozygous knockout mice die during embryonic development with defects in the nervous system.[8] Heterozygous mice survive to adulthood, and 14–20% develop medulloblastoma several months after birth.[8,9] Histological and marker expression analysis of the brain tumor has revealed that they closely resemble human medulloblastoma,[9] and similar to human cases, the origin of medulloblastoma in ptch1 mice is thought to be residual EGL cells that failed to exit proliferation.[10] Activation of the Shh pathway has also been confirmed in the tumors of ptch1 mice,[9] and this mouse model is equivalent to the SHH group in human cases. While the study of the molecular mechanism underlying medulloblastoma formation has progressed, few studies on the modifying effects of chemicals on tumor development have been conducted.

Although ptch1 mice are a valuable model for studying medulloblastoma, the low frequency and long latency for tumor development are disadvantages for detection of the modulatory effects on medulloblastomas, especially in the case of tumor suppressive compounds. Previous reports showed that neonatal irradiation dramatically increased the incidence of medulloblastoma, and it has been suggested that tumorigenesis in ptch1 mice follows a multi-step process.[10–12] So far, medium-term carcinogenicity bioassays based on the multi-step cancer development (initiation promotion model) have been established in many organs to detect modifying effects on tumor development in a short term.[13,14] *N*-ethyl-*N*-nitrosourea (ENU) is a very common initiator and is known to induce nervous system tumors including medulloblastoma in newborn mice.[15,16] Therefore, to increase the incidence and decrease the time required for tumor development, we attempted to induce medulloblastoma using ENU in ptch1 mice.

Materials and Methods

Mice. Ptch1 heterozygous knockout mice, generated by replacing exon 1 and 2 of the *ptch1* gene with a LacZ/neomycin cassette,[8] were obtained from The Jackson Laboratory (Bar Harbor, ME, USA) and maintained in our laboratory. They were housed in polycarbonate cages with wood chip bedding and kept in an air-conditioned animal room with basal diet (CRF-1; Oriental Yeast, Tokyo, Japan) and tap water available *ad libitum*.

Experimental design. Twenty-five dams were used in experiment 1. Ptch1 mice and their wild-type (WT) littermates received a single intraperitoneal injection of ENU (Nacalai Tesque, Kyoto, Japan) dissolved in saline. The highest dose selected was 100 mg/kg based on a previous study,[15,16] and 50 and 10 mg/kg were set as medium and low doses, respectively. Postnatal day 1 (d1) or 4 (d4) was chosen as administration day because they are periods of active proliferation in

[4]To whom correspondence should be addressed.
E-mail: mtakahashi@nihs.go.jp

doi: 10.1111/cas.12006

Table 1. The number and survival rate (%) of ptch1 and wild-type mice examined at 12 weeks of age

Administration day	ENU (mg/kg)	No. of litters	Ptch1 No. (%)	Wild-type No. (%)
–	0 (Control)	5	16 (93.8)	11 (90.9)
d1	10	3	15 (100)	5 (100)
	50	3	15 (93.3)	8 (100)
	100	5	23 (87.0)	5 (100)
d4	10	3	10 (100)	9 (100)
	50	3	10 (90.0)	11 (100)
	100	3	14 (85.7)	6 (83.3)

d1, postnatal day 1; d4, postnatal day 4; ENU, *N*-ethyl-*N*-nitrosourea.

the EGL. Intact mice were used as the controls. Each group was composed of at least 10 ptch1 mice and five WT mice from three to five dams (Table 1). Daily observation for clinical signs and mortality was conducted throughout the study. We set the duration as 12 weeks, because mortality caused by malignant lymphoma increased after 13 weeks of age in a preliminary study. At 12 weeks of age, all animals were subjected to autopsy under deep isoflurane anesthesia. The brains, thymus, spleen and macroscopic lesions were removed and fixed in neutrally-buffered 10% formalin. The tissues were routinely processed for paraffin embedding, sectioned and stained with hematoxylin and eosin.

In experiment 2, ptch1 and WT mice from 16 dams received 100 mg/kg of ENU intraperitoneally on d1 or d4, and the brains of each of the 9–13 mice were removed on d4, 7, 14 or 21. For comparison, the brains from 12 intact mice including both genotypes were also collected at the same time point, respectively, and the tissues were processed routinely for histological examination.

The animal protocol was reviewed and approved by the Animal Care and Use Committee of the National Institute of Health Sciences, Japan.

Histopathology. All cerebella were examined in midsagittal section. Based on a previous report,[17] the stage of neoplastic lesions in the cerebellum was classified according to the size as follows: hyperproliferation of EGL, micronodule, nodule, microtumor and full-blown tumor (Fig. 1).

Persistent EGL cells were classified into the focal lesion and the diffuse or zonal lesions, according to type of distribution. The degrees of focal lesions were divided as follows: grade 1, only one to two very small clusters consisting of about 10 cells; grade 2, a few clusters consisting of about 10–30 cells; and grade 3, several clusters consisting of 30 cells or more in the midsagittal section of the cerebellum. Diffuse lesions were divided as follows: grade 1, persistent EGL cells distributed diffusely in a part of the cerebellum; and grade 2, persistent EGL cells distributed diffusely in most areas of the cerebellum. In addition, when the cell clusters were observed parallel to the granular layer, we classified the lesions into zonal type.

Morphometric assessment. Photomicrographs of midsagittal sections of the cerebellum were taken with a digital camera attached to a microscope (DP71; Olympus, Tokyo, Japan), and measurement was performed using image analysis software (WinROOF, Version 5.7.1; Mitani, Tokyo, Japan). The areas of the cerebellum and granular layer were measured for each genotype, and the animals with a large tumor were eliminated. The average width of the EGL of each mouse was determined by tenth measurements selected at random from the entire cerebellum. Because the width did not differ according to genotype, we counted the values of both mice together.

Statistical analysis. As for data of the areas of the cerebellum and granular layer, values of the d1-treated and d4-treated groups were compared with the corresponding controls by one-way ANOVA or the Kruskal–Wallis test. When statistically significant differences were detected, Dunnett's multiple comparisons test was used for comparison between the control and treatment groups. Incidence of histopathological findings was compared using Fisher's exact probability test. Width of EGL was analyzed by the Student's or Welch's *t*-test following a test for equal variance.

Results

Most mice were asymptomatic throughout the study. Eight ptch1 mice and two WT mice were found dead or moribund. Hydrocephalus was found in three ptch1 mice, and the cause of death in the other cases could not be determined. At 12 weeks of age, there were no intergroup differences in survival rate in both groups (Table 1). A significant difference was not detected in final body weight (data not shown).

Reduction of cerebellar size was apparent at 50 mg regardless of genotype (Fig. 2), and morphometric analysis revealed a significant decrease in the areas of the cerebellum and granular layer in the groups treated with 50 or 100 mg of ENU (Fig. 3).

The incidence of medulloblastoma in ptch1 mice of the control group was 19% (3/16) (Fig. 4). In contrast, 11 of 15 (73%) and six of 10 (60%) mice developed medulloblastoma in the groups receiving 10 mg on d1 or d4, respectively. At 50 mg, medulloblastoma occurred in seven of 15 (47%) mice treated on d1 and in two of 10 (20%) mice treated on d4. At 100 mg, the tumor incidence was 27% (6/22) in d1-treated mice and 29% (4/14) in d4-treated mice. Most were regarded as an early stage of medulloblastoma, and a significant increase in the incidence was detected only in the groups receiving 10 mg. In WT mice, there was no medulloblastoma occurrence in either group.

As previously reported, focal lesions of persistent EGL in subpial position were common in ptch1 mice and occasionally found in WT mice (Fig. 5A). The incidence and degree of subpial EGL foci were not greatly influenced by ENU treatment (Fig. 5E). In contrast, the persistent EGL cells were distributed diffusely in the molecular layer in mice receiving ENU at 10 and 50 mg (Fig. 5B), and the persistent EGL cells showed a

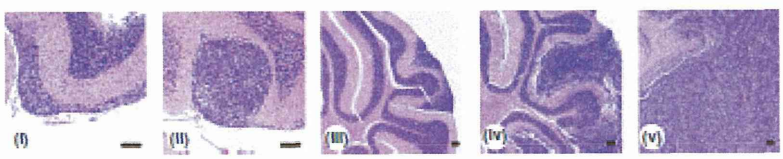

Fig. 1. Neoplastic lesions in the cerebellum. Neoplastic lesions in the cerebellum were classified according to size as follows; (i) hyperproliferation of external granular layer, (ii) micronodule, (iii) nodule, (iv) microtumor and (v) full-blown tumor. Hematoxylin and eosin section. Bar, 100 μm.

doi: 10.1111/cas.12006

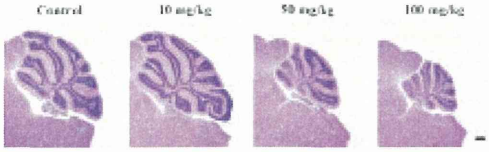

Fig. 2. Changes in the cerebellar size of ptch1 mice receiving *N*-ethyl-*N*-nitrosourea on postnatal day 1. Bar, 500 μm.

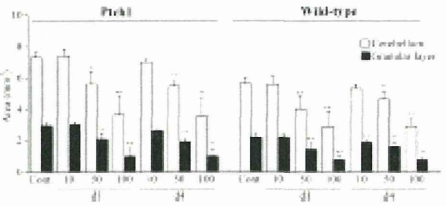

Fig. 3. Areas of the cerebellum and granular layer in ptch1 and wild-type (WT) mice. Significantly different from the control group at $^{*}P < 0.05$ and $^{**}P < 0.01$, respectively. Significantly different from the control group at $^{\dagger\dagger}P < 0.01$.

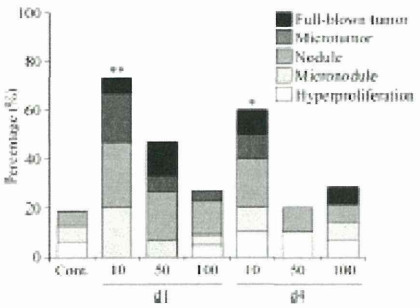

Fig. 4. Total incidence of medulloblastoma in ptch1 mice. Significantly different from the control group at $^{*}P < 0.05$ and $^{**}P < 0.01$, respectively.

zonal distribution parallel to the granular layer in the molecular layer at 100 mg in both ptch1 and WT mice (Fig. 5C,F). The persistent EGL cells of focal and diffuse types were well-differentiated, and cellular atypia and mitosis were rarely seen, unlike in medulloblastoma cells. In accordance with the morphometric analysis, reduction of the number of granule cells was histologically apparent starting at 50 mg. Also, misalignment of Purkinje cells was noted from 50 mg regardless of genotype (Fig. 5D,G).

Other than medulloblastoma, there was no occurrence of neural tumors in ptch1 and WT mice. Thymic lymphoma, which is induced by ENU in mice, was increased dose-dependently. The incidence in ptch1 mice was 14% in the group receiving 100 mg on d1 and 10% and 50% in the groups receiving 50 and 100 mg on d4, respectively. Also in WT mice, thymic lymphoma occurred in 25% and 40% of the d1-treated mice at 50 and 100 mg, respectively, and in 11%, 18% and 67% of the d4-treated mice at 10, 50 and 100 mg, respec-

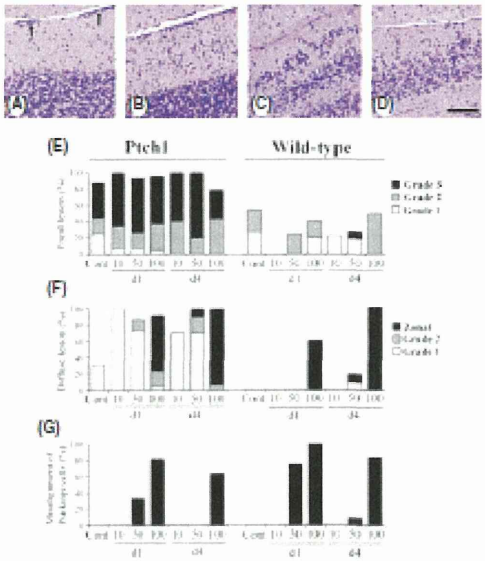

Fig. 5. Histopathological findings observed in cerebellar cortex. Morphologic changes observed in the cerebellar cortex of ptch1 mice, and the incidence of these lesions in ptch1 and wild-type (WT) mice. (A) Focal lesions of persistent external granular layer (EGL) in subpial position (arrows) observed in ptch1 mice of the control group (grade 2). (B) The lesions of persistent EGL cells distributed diffusely in the molecular layer of ptch1 mice receiving 10 mg of *N*-ethyl-*N*-nitrosourea (ENU) on postnatal day 1 (d1) (grade 1). (C) The persistent EGL cells showed zonal distribution parallel to the granular layer in the molecular layer of ptch1 mice receiving 100 mg of ENU on postnatal day 4 (d4). (D) Misalignment of Purkinje cells observed in ptch1 mice receiving 100 mg of ENU on d1. Hematoxylin and eosin section. Bar, 100 μm. The incidence of focal lesions of persistent EGL in subpial position (E), the diffuse lesions of persistent EGL in the molecular layer (F), and misalignment of Purkinje cells (G).

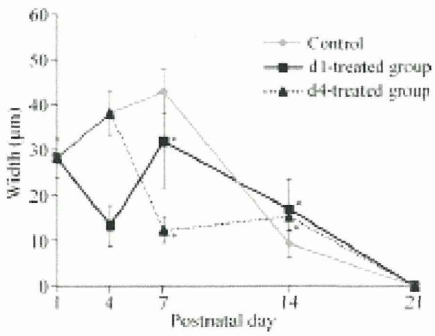

Fig. 6. The width of the external granular layer in the developing cerebellum of mice receiving 100 mg of *N*-ethyl-*N*-nitrosourea on postnatal day 1 (d1) or postnatal day 4 (d4). Significantly different from the control group at $^{*}P < 0.01$.

tively. Hydrocephalus and rhabdomyosarcomas, which are known to occur spontaneously in ptch1 mice, were found in three ptch1 mice each, and ENU did not affect their incidence.

In experiment 2, there were no intergroup differences in body weight throughout the study (data not shown). The width of EGL in the control group peaked at postnatal day 7 and then decreased gradually and disappeared at postnatal day 21 (Fig. 6). In mice receiving 100 mg on d1, the width of EGL was strikingly reduced at d4. Then, EGL considerably recovered at d7 and was wider than the control group at d14. Similarly, the width of EGL in mice of the d4-treated group was significantly decreased at d7 and then became wider than that in the control at d14. But, the degree of recovery after damage by ENU was milder than that in the d1-treated group. Misalignment of Purkinje cells was apparent, especially in the d1-treated group. A difference in EGL development between ptch1 and WT mice was not observed in the present study.

Discussion

Medulloblastomas were observed frequently in 12-week-old ptch1 mice receiving 10 mg of ENU. In ptch1 mice, preneoplastic lesions of medulloblastoma were seen at a high incidence at 2–3 weeks of age, and these lesions spontaneously regressed or matured by 10 weeks of age.[17,18] Therefore, in the present study, the lesions observed at 12 weeks of age were regarded as selected lesions that directly led to tumor, although most lesions were regarded as an early stage of medulloblastoma. It is believed that ptch1 haploinsufficiency alone is not sufficient to induce tumor formation and that additional genetic lesions are required for tumorigenesis.[9,11] Because ENU is a multipotent genotoxic carcinogen, ENU possibly enhanced tumorigenesis by increasing DNA damage similar to radiation and p53 inactivation.[7,11,19]

As for the dose of ENU, 10 mg appeared to be appropriate for medulloblastoma induction based on the high incidence of medulloblastoma and low impact on cerebellum structure and lymphoma. In contrast, 50 and 100 mg of ENU reduced the size of the cerebellum, and significant induction of medulloblastoma was not observed. In experiment 2, EGL cells, a possible origin of medulloblastoma, were strikingly decreased after 100 mg of ENU. Consequently, the damage of ENU to EGL cells was so severe at a high dose that stockpiles of the damaged EGL cells to develop medulloblastoma could be limited.

Timing of administration is also an important factor for medulloblastoma induction, and in the present study, d1 was more effective than d4. In experiment 2, the response to ENU damage was different between d1 and d4-treatment. The strong recovery of EGL after ENU injection that was observed in the d1-treated group may be a reason for enhanced tumor induction. A previous study demonstrated that EGL cells at d1 showed resistance to radiation-induced cell death and p53 induction compared with EGL cells at d10, despite evident ongoing proliferation at both d1 and d10.[12] Such differences in cellular response to ENU damage might also contribute to the increased tumor induction in the d1-treated group.

Focal lesions of persistent EGL in the subpial position were common in ptch1 mice and occasionally found in WT mice. In addition, the lesions of persistent EGL cells distributed diffusely or zonally in the molecular layer were induced by ENU in both mice. But, the incidence of persistent EGL cells did not correlate with medulloblastoma induction. Persistent EGL has been observed in other mutant mice, and it is believed that persistence of the EGL alone is not sufficient for tumorigenesis because none of the mutant mice showing persistent EGL, other than ptch1 mice develop medulloblastoma.[20] Furthermore, morphological alterations like ectopic EGL cells were induced by chemicals such as methyl-azoxy-methanol and cisplatin during cerebellar histogenesis in rats and mice, along with disappearance of the basket cells or damage of glial fibers.[21,22] Because persistence of the EGL was found in both ptch1 and WT mice, this phenomenon may occur independently of the Shh-Ptch pathway, although damage of glia and basket cells was not apparent in our study. Misalignment of Purkinje cells was reported in rat cerebellum following prenatal exposure to X-irradiation, and the decrease in Reelin, which is expressed in the granule cell at a high level and helps regulating processes of neuronal migration and positioning in the developing brain, was thought to be a possible cause.[23] Therefore, misalignment of Purkinje cells observed in our study also may result from a marked decrease in EGL cells damaged by ENU.

Currently, human medulloblastomas are classified as four distinct subtypes by genomic approaches,[5,6] and future development of therapeutics and new drugs for medulloblastoma should take account of these subtypes. Tumors of ptch1 mice are thought to be equivalent for those of the SHH group in human, therefore, our model will be a useful tool for testing new drugs targeting the Shh pathway. Additionally, cerebellar development occurring after birth in mice is of good benefit for investigation of the effects of chemical exposure during development on medulloblastoma. Because medulloblastoma of ptch1 mice resembles human cases in histology, marker expression and cell origin, our model will be informative for human risk assessment of environmental chemicals and new drugs during development. In contrast, it should be recognized that ptch1 mouse is unsuitable for the research of medulloblastoma other than the SHH group. Also, this model might not be applicable for elucidation of onset of human medulloblastoma in some cases, because our model is developed for rapid screening of environmental chemicals and new drugs and there might be some differences between induced and spontaneous tumors at the molecular level.

In summary, ENU is available for the induction of medulloblastoma in ptch1 mice, and 10 mg of ENU administered on d1 was an appropriate dosing condition. Induction of medulloblastoma by ENU may be a good model for studying modifier effects on medulloblastoma tumorigenesis because this method allows for high tumor frequency and shorter latency and there was no occurrence of neural tumors other than medulloblastoma in the brain. This model will be helpful for human risk assessment of environmental chemicals and new drugs targeting the Shh pathway.

Acknowledgment

We thank Ms Tomomi Morikawa, Ayako Kaneko and Yoshimi Komatsu for technical assistance in conducting the animal study. This study was supported by Health and Labour Sciences Research Grants, Research on Risk of Chemical Substances, Ministry of Health, Labour and Welfare, Japan (H22-Toxicol-003).

Disclosure Statement

The authors have no conflict of interest.

doi: 10.1111/cas.12006